mediated by the other receptor intact, which may be sufficient for Fos induction. We therefore decided to inhibit all of the PG-mediated pathways by treatment with indomethacin and examine its effects on Fos induction. Indeed, in keeping with previous studies (9, 10), the treatment with indomethacin significantly decreased the number of LPS-induced Fos-IR-positive cells in the PVN (Fig. 2*B*). We therefore administered ONO-8713 to EP3$^{-/-}$ mice to block both EP1 and EP3 in these animals and measured c-Fos expression in the PVN. Intriguingly, treatment of EP3$^{-/-}$ mice with ONO-8713 resulted in a decrease in the number of Fos-IR-positive cells to an extent comparable to that found in indomethacin-treated wild-type mice (Fig. 2*B*). Double immunostaining with c-Fos and CRH antibodies revealed that most c-Fos-positive neurons in the PVN of wild-type mice were CRH-immunoreactive (Fig. 2*C*). Thus, c-Fos reduction in EP3$^{-/-}$ mice with ONO-8713 is likely to occur in CRH-containing neurons in the PVN.

Because the above c-Fos assay measured the number of Fos-IR-positive cells irrespective of its amount in each cell, we next quantified the amount of c-Fos mRNA by RT-PCR. Because of the detection threshold of this method, we treated mice with a high dose of LPS (2.5 mg/kg i.p.) and subjected the whole hypothalamus to the analysis. The LPS injection indeed induced a significant amount of c-Fos mRNA in the hypothalamus, and this induction was impaired in both EP1$^{-/-}$ and EP3$^{-/-}$ mice (Fig. 2*D*). These results strongly suggest that both EP1 and EP3 mediate LPS-induced activation of the hypothalamus. This is consistent with a view that a pathway mediated by either EP1 or EP3 alone can activate neurons in the PVN to some extent, but the synergistic activation by both pathways is required for PVN activation sufficient for ACTH release.

We next extended the Fos-IR analysis to other regions known to be activated in response to LPS in rats (9, 10, 29). They include the central nucleus of the amygdala (CeA), the nucleus of the solitary tract (NTS), and the ventrolateral medulla (VLM). A sizable number of neurons were responsive to LPS in CeA of wild-type mice (Fig. 2*E*). Notably, EP1$^{-/-}$ mice showed a significant reduction in the number of Fos-IR-positive cells (Fig. 2*E*), indicating the involvement of EP1 in LPS-induced activation of CeA neurons. A small decrease in c-Fos expression also was noted in NTS of EP1$^{-/-}$ mice compared with wild-type mice, but the difference was not statistically significant (Fig. 2*F*). No decrease was found in either region of EP3$^{-/-}$ mice. In the VLM, only very sparse c-Fos staining was observed in LPS-treated wild-type mice (data not shown), which precluded quantitative comparison among mice of different genotypes. A similar c-Fos analysis also was performed in EP2$^{-/-}$ and EP4$^{-/-}$ mice. However, no difference was found in any of the above regions of EP2$^{-/-}$ or EP4$^{-/-}$ mice as compared with wild-type or control mice of identical genetic background (data not shown).

EP1 Is Localized at the Synapse on CRH-Containing Neurons in the PVN. The above findings demonstrated that EP1 and EP3 distinctly but synergistically regulate LPS-induced CNS responses. Localization of EP3 in the brain already was studied extensively by both *in situ* hybridization (20, 30, 31) and immunohistochemistry (32). Whereas the former studies detected little hybridization signals for EP3 mRNA in the PVN, the latter study reported moderate EP3-IR in the neuropil in this area, suggesting that EP3 may be present at terminals of neurons projecting to this area. On the other hand, *in situ* hybridization studies of EP1 (20, 33) revealed weak and diffuse signals in the PVN and provide no information on its expression in CeA. No systematic analysis of EP1 immunostaining in the brain is yet available. We therefore examined EP1 expression in these areas by immunohistochemistry using an anti-EP1 antibody (24).

We first verified the specificity of this antibody by using cultured cells expressing cloned EP1 or EP3 receptor. This

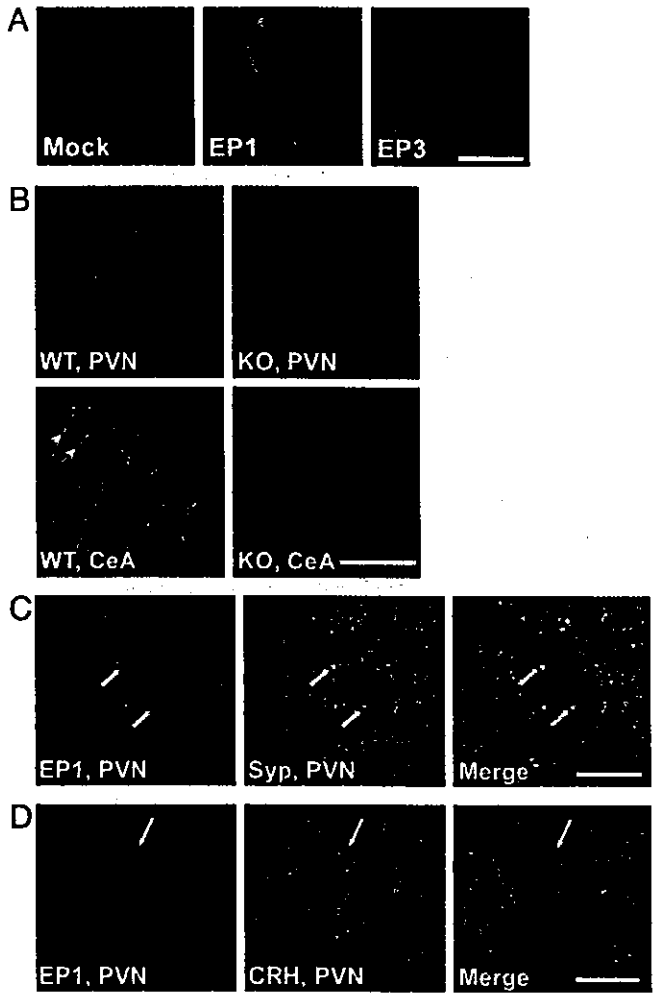

Fig. 3. Localization of EP1 in PVN and CeA. (*A*) Specificity of the antibody. EP1-IR of COS-7 cells expressing LacZ (Mock), EP1, or EP3 is shown. (Bar = 50 μm.) (*B*) EP1-IR in PVN and CeA of wild-type (WT) and EP1$^{-/-}$ (KO) mice. (Bar = 200 μm for PVN and 25 μm for CeA.) (*C*) Double immunostaining of EP1 and synaptophysin (Syp). Arrows show the colocalized signals of EP1-IR and Syp-IR. (Bar = 20 μm.) (*D*) Double immunostaining of EP1 and CRH. (Bar = 10 μm.)

antibody stained COS-7 cells expressing EP1 and not cells transfected with either LacZ or EP3 (Fig. 3*A*). Brain sections then were subjected to staining with this antibody. As shown in Fig. 3*B*, EP1-IR was detected in the PVN and CeA of wild-type mice as punctate signals. On the other hand, little, if any, signal was found in the corresponding brain regions of EP1$^{-/-}$ mice, indicating that the IR detected in wild-type mice represents EP1. Double immunostaining showed that most of EP1-IR puncta in the PVN and CeA were colocalized with those stained for synaptophysin (Fig. 3*C* and data not shown). Furthermore, some, if not all, EP1-IR puncta were clearly juxtaposed with CRH-IR-positive neurons in the PVN (Fig. 3*D*). These data suggest that EP1 is present at the synapses on CRH-containing neurons in the PVN.

Localization of Enzymes in PGE Synthesis. Given the local action of PGs, the site of PGE_2 synthesis is critical to understand where and how EP1 and EP3 are activated. We therefore examined the localization of enzymes responsible for PGE_2 synthesis, namely, COX-1, COX-2, and mPGES-1, in the PVN by immunohistochemistry. As reported (21), COX-1-IR was expressed constitutively on glia-like cells in the PVN (Fig. 4) as well as other brain

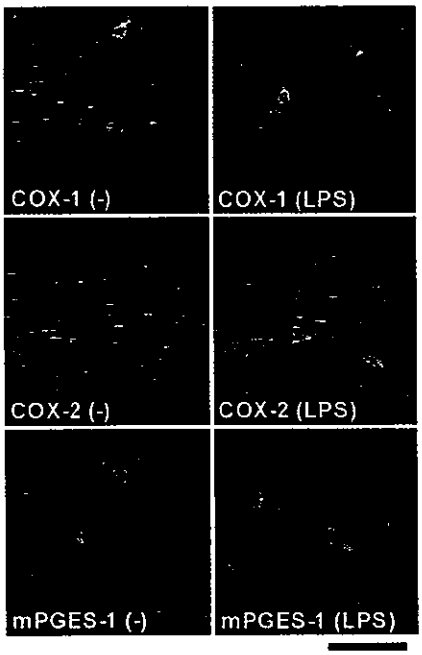

Fig. 4. Localization of enzymes for PGE_2 synthesis in the PVN. Wild-type mice were treated with or without LPS, and the brain was isolated and subjected to the analysis 3 h after injection. (Bar = 30 μm.)

areas (data not shown) of mice with or without LPS. In contrast, COX-2-IR was inducible and was detectable in the PVN only at 3 h, but not at 1 h, after LPS challenge as a pattern reminiscent of blood vessels (Fig. 4 and data not shown). mPGES-1 also was stained in the vessel-like structure within the PVN, but the level of its expression appeared unaltered with or without LPS challenge (Fig. 4). This constitutive expression of mPGES-1 was in contrast to the previous reports that it is induced by LPS challenge (22, 34). The specificity of this mPGES-1-IR was confirmed by using two independent mPGES-1 antibodies, which yielded overlapped staining patterns (data not shown).

Discussion

A role of PGs in the HPA axis activation induced by LPS or inflammatory cytokines has long been suggested (6–11). However, the importance and identity of the PG-mediated process in this response have remained to be examined (2). This is probably because pharmacological effects of NSAIDs were variable and because specific drugs for each PG receptor subtype were not available. With the use of knockout mice deficient in each of the four PGE receptor subtypes, we showed that LPS-induced ACTH release was impaired in mice deficient in either EP1 or EP3 but not in those lacking either EP2 or EP4 (Fig. 1). This study thus unambiguously demonstrated the direct involvement of PGE_2 in LPS-induced HPA axis activation. Given the specific involvement of EP3 but not EP1 in LPS-induced fever generation (15), this study further suggests that at least some PG-mediated mechanisms are different in fever generation and ACTH release induced by LPS. Our findings appear contradictory to the current proposal that EP4 may be a primary PGE receptor mediating the HPA axis activation (35). This proposal is based on the findings that LPS injection induces EP4 in CRH-containing neurons in rat PVN (20, 35). Our results, together with the finding that the EP4 induction is sensitive to NSAID treatment (35), suggest that the EP4 induction is secondary to other PG-mediated processes.

Given the primary role of EP1 and EP3 in ACTH release, we further addressed the site at which EP1 and EP3 act in the HPA axis. The PVN and the pituitary are two critical sites regulating the HPA axis. By using c-Fos as a marker for neuronal activation, we showed that EP1- and EP3-mediated pathways are likely to converge onto the PVN (Fig. 2), although our study did not rule out their involvement in the pituitary. Given that a PG-dependent component of ACTH release is abolished in both $EP1^{-/-}$ and $EP3^{-/-}$ mice (Fig. 1), the synergistic action of EP1 and EP3 appears to be required for PVN activation for ACTH release at least under our experimental conditions. However, we do not exclude a possibility that these two pathways may work differently in time and/or in response to different doses of LPS.

Then, what are the neuronal substrates for the EP1- and EP3-mediated PVN activation? There are multiple brain areas that could regulate the PVN directly or indirectly (36). Forebrain limbic areas, including ventral subiculum, prefrontal cortex, and CeA, are thought to regulate the PVN through intermediate areas such as the bed nucleus of stria terminalis, the preoptic area, and other hypothalamic nuclei. In parallel, the medullary catecholaminergic cell groups such as the VLM directly project to and activate the PVN. Our c-Fos study (Fig. 2) revealed that the number of LPS-induced Fos-IR-positive cells was diminished in CeA of $EP1^{-/-}$ mice, thus implicating the EP1 action in regulating CeA neurons. Consistently, EP1-IR was detected at synapses on CeA neurons (data not shown). On the other hand, the preoptic area and the VLM are possible sites of the EP3 action, because they express EP3 (30–32) and have been suggested to be involved in PGE-mediated HPA axis activation (7, 9, 10, 37). In addition to the PVN activation from other areas, it is also possible that PGs act within the PVN. Indeed, both EP1 and EP3 are distributed in the neuropil of the PVN (Fig. 3 and ref. 32).

Then, what is the cellular mechanism of EPs to activate PVN neurons? Our immunostaining revealed that EP1-IR is localized at the synapse on PVN and CeA neurons (Fig. 3 and data not shown). This finding implicates EP1 in direct regulation of synaptic transmission in the PVN and CeA. It is also reported that EP3 regulates γ-aminobutyrate (GABA)ergic synaptic transmission by a presynaptic mechanism in the supraoptic nucleus (38). GABAergic inputs from similar areas are also found on neurons in the PVN (39). Therefore, EP1 and EP3, which are expressed in neurons, may directly regulate synaptic connections that serve for HPA axis activation. EP1 is present at only a small population of synapses on CRH-containing neurons in the PVN, indicating that EP1 regulates a distinct type of synaptic inputs to CRH-containing neurons. The origin of these projections remains to be clarified.

PGs are formed locally and act in the vicinity of their synthesis (5). It generally is believed that PG synthesis in response to LPS or inflammatory cytokines is catalyzed by COX-2 and mPGES-1 induced in brain vasculature (22, 34). We examined this issue in the PVN and confirmed that COX-2 is induced and coexpressed with mPGES-1 in brain vasculature at 3 h after injection of LPS (Fig. 4), although we found that mPGES-1 is constitutively expressed without LPS stimulation. It is possible that these enzymes catalyze the formation of PGE_2 in the PVN. It was reported previously that PGE_2 is produced significantly in the PVN upon IL-1β injection (40). However, induction of COX-2 in endothelial cells was not observed as early as 1 h after the injection. On the other hand, we observed constitutive expression of COX-1 in glia-like cells in the PVN. There are several reports indicating the involvement of glia in PG production in the brain. Microglial cells produce a large amount of PGs when incubated with LPS *in vitro* (41). PG synthesis associated with neuronal activation also was reported in astrocytes (42). Furthermore, COX-2 is constitutively expressed and localized to the somatodendritic region of excitatory neurons in the cerebral

cortex, the hippocampus (including subiculum), and the ai dala (43, 44), all of which may contribute to HPA axis activ (36). Therefore, it is possible that multiple pathways for synthesis, each of which is activated in a different temp pattern in response to LPS, contribute to PG-mediated HPA activation.

In summary, we demonstrated that two distinct path mediated by EP1 and EP3 are activated in response to LPS are required for LPS-induced PVN activation in the HPA This knowledge will help further clarify novel neural me nisms implicated in sickness-induced CNS symptoms.

We thank A. Shimatsu, Y. Sugimoto, and E. Segi for helpful discussions and comments, K. Matsumura for advice on the immunohistochemistry of COX-1, COX-2, and mPGES-1, N. Eguchi for a guinea pig anti-mPGES-1 antibody, C. Hamada for advice on statistical analyses, K. Deguchi, N. Kitagawa, and T. Fujiwara for animal care and breeding, and T. Arai and H. Nose for secretarial assistance. This work was supported in part by Grants-in-Aid for Scientific Research from the Ministry of Education, Science, Sports and Culture of Japan and by grants from the Organization for Pharmaceutical Safety and Research of Japan, the Mitsubishi Foundation, and the ONO Medical Research Foundation. T.F. is a postdoctoral fellow of the Japan Society for the Promotion of Science.

1. Kent, S., Bluthé, R.-M., Kelley, K. W. & Dantzer, R. (1992) *Trends Pharm Sci.* **13**, 24–28.
2. Turnbull, A. V. & Rivier, C. L. (1999) *Physiol. Rev.* **79**, 1–71.
3. Kopin, I. J. (1995) *Ann. N.Y. Acad. Sci.* **771**, 19–30.
4. Johnson, E. O., Kamilaris, T. C., Chrousos, G. P. & Gold, P. W. (*Neurosci. Biobehav. Rev.* **16**, 115–130.
5. Narumiya, S., Sugimoto, Y. & Ushikubi, F. (1999) *Physiol. Rev.* **79**, 1193–
6. Morimoto, A., Murakami, N., Nakamori, T., Sakata, Y. & Watanabe, T. (*J. Physiol. (London)* **411**, 245–256.
7. Katsuura, G., Arimura, A., Koves, K. & Gottschall, P. E. (1990) *Am. J. Pl* **258**, 163–171.
8. Rivier, C. & Vale, W. (1991) *Endocrinology* **129**, 384–388.
9. Lacroix, S. & Rivest, S. (1997) *J. Comp. Neurol.* **387**, 307–324.
10. Ericsson, A., Arias, C. & Sawchenko, P. E. (1997) *J. Neurosci.* **15**, 7166–
11. Nasushita, R., Watanobe, H. & Takebe, K. (1997) *Prostaglandins Leukot Essent. Fatty Acids* **56**, 165–168.
12. Murata, T., Ushikubi, F., Matsuoka, T., Hirata, M., Yamasaki, A., Sugi Y., Ichikawa, A., Aze, Y., Tanaka, T., Yoshida, N., *et al.* (1997) *Natur* 678–682.
13. Sugimoto, Y., Yamasaki, A., Segi, E., Tsuboi, K., Aze, Y., Nishimura, T., H., Yoshida, N., Tanaka, T., Katsuyama, M., *et al.* (1997) *Science* **277**, 681
14. Segi, E., Sugimoto, Y., Yamasaki, A., Aze, Y., Oida, H., Nishimura, T., M T., Matsuoka, T., Ushikubi, F., Hirose, M., *et al.* (1998) *Biochem. Biophys Commun.* **246**, 7–12.
15. Ushikubi, F., Segi, E., Sugimoto, Y., Murata, T., Matsuoka, T., Kobayasl Hizaki, H., Tuboi, K., Katsuyama, M., Ichikawa, A., *et al.* (1998) *Natur* 281–284.
16. Hizaki, H., Segi, E., Sugimoto, Y., Hirose, M., Saji, T., Ushikubi, F., Mats T., Noda, Y., Tanaka, T., Yoshida, N., *et al.* (1999) *Proc. Natl. Acad. Sci.* **96**, 10501–10506.
17. Matsuoka, T., Hirata, M., Tanaka, H., Takahashi, Y., Murata, T., Kabas K., Sugimoto, Y., Kobayashi, T., Ushikubi, F., Aze, Y., *et al.* (2000) *Scienc* 2013–2017.
18. Takao, T., Nakata, H., Tojo, C., Kurokawa, H., Nishioka, T., Hashimoto, De Souza, E. (1994) *Brain Res.* **649**, 265–270.
19. Watanabe, K., Kawamori, T., Nakatsuji, S., Ohta, T., Ohuchida, S., Yamai H., Maruyama, T., Kondo, K., Ushikubi, F., Narumiya, S., *et al.* (2000) *C Lett.* **156**, 57–61.
20. Oka, T., Oka, K., Scammell, T. E., Lee, C., Kelly, J. F., Nantel, F., Elm J. E. & Saper, C. B. (2000) *J. Comp. Neurol.* **428**, 20–32.
21. Li, S., Wang, Y., Matsumura, K., Ballou, L. R., Morham, S. G. & Bali C. M. (1999) *Brain Res.* **825**, 86–94.
22. Yamagata, K., Matsumura, K., Inoue, W., Shiraki, T., Suzuki, K., Yasuda, S., Sugiura, H., Cao, C., Watanabe, Y. & Kobayashi, S. (2001) *J. Neurosci.* **21**, 2669–2677.
23. Lazarus, M., Kubata, B. K., Eguchi, N., Fujitani, Y., Urade, Y. & Hayaishi, O. (2002) *Arch. Biochem. Biophys.* **397**, 336–341.
24. Bhattacharya, M., Peri, K. G., Almazan, G., Ribeiro-da-Silva, A., Shichi, H., Durocher, Y., Abramovitz, M., Hou, X., Varma, D. R. & Chemtob, S. (1998) *Proc. Natl. Acad. Sci. USA* **95**, 15792–15797.
25. Calogero, A. E., Gallucci, W. T., Kling, M. A., Chrousos, G. P. & Gold, P. W. (1989) *Brain Res.* **505**, 7–11.
26. Fujiwaki, R., Hata, K., Nakayama, K., Moriyama, M., Iwanari, O., Katabuchi, H., Okamura, H., Sakai, E. & Miyazaki, K. (2002) *Int. J. Cancer* **99**, 328–335.
27. Rivier, C. (1994) in *Bilateral Communication Between the Endocrine and Immune Systems*, ed. Grossman, C. (Springer, New York), Vol. 7, pp. 183–196.
28. Shin, C., McNamara, J. O., Morgan, J. I., Curran, T. & Cohen, D. R. (1990) *J. Neurochem.* **55**, 1050–1055.
29. Elmquist, J. K., Scammell, T. E., Jacobson, C. D. & Saper, C. B. (1996) *J. Comp. Neurol.* **371**, 85–103.
30. Sugimoto, Y., Shigemoto, R., Namba, T., Negishi, M., Mizuno, N., Narumiya, S. & Ichikawa, A. (1994) *Neuroscience* **62**, 919–928.
31. Ek, M., Arias, C., Sawchenko, P. & Ericsson-Dahlstrand, A. (2000) *J. Comp. Neurol.* **428**, 5–20.
32. Nakamura, K., Kaneko, T., Yamashita, Y., Hasegawa, H., Katoh, H. & Negishi, M. (2000) *J. Comp. Neurol.* **421**, 543–569.
33. Batshake, B., Nilsson, C. & Sundelin, J. (1995) *Eur. J. Biochem.* **231**, 809–814.
34. Ek, M., Engblom, D., Saha, S., Blomqvist, A., Jakobsson, P. & Ericsson-Dahlstrand, A. (2001) *Nature* **410**, 430–431.
35. Zhang, J. & Rivest, S. (2000) *J. Neurochem.* **74**, 2134–2145.
36. Herman, J. P. & Cullinan, W. E. (1997) *Trends Neurosci.* **20**, 78–84.
37. Scammell, T. E., Elmquist, J. K., Griffin, J. D. & Saper, C. B. (1996) *J. Neurosci.* **16**, 6246–6254.
38. Shibuya, I., Setiadji, S. V., Ibrahim, N., Harayama, N., Maruyama, T., Ueta, Y. & Yamashita, H. (2002) *J. Neuroendocrinol.* **14**, 64–72.
39. Armstrong, W. E. (1995) in *The Rat Nervous System*, ed. Paxinos, G. (Academic, San Diego), 2nd Ed., pp. 377–390.
40. Watanobe, H. & Takebe, K. (1994) *Neuroendocrinology* **60**, 8–15.
41. Minghetti, L. & Levi, G. (1998) *Prog. Neurobiol.* **54**, 99–125.
42. Bezzi, P., Carmingnoto, G., Pasti, L., Vesce, S., Rossi, D., Lodi Rizzini, B., Pozzan, T. & Volterra, A. (1998) *Nature* **391**, 281–285.
43. Breder, C. D., Dewitt, D. & Kraig, R. P. (1995) *J. Comp. Neurol.* **355**, 296–315.
44. Kaufmann, W. E., Worley, P. F., Pegg, J., Bremer, M. & Isakson, P. (1996) *Proc. Natl. Acad. Sci. USA* **93**, 2317–2321.

J Am Soc Nephrol 14: 1154–1163, 2003

Angiogenic Protein Cyr61 is Expressed by Podocytes in Anti-Thy-1 Glomerulonephritis

KAZUTOMO SAWAI, KIYOSHI MORI, MASASHI MUKOYAMA, AKIRA SUGAWARA, TAKAYOSHI SUGANAMI, MASAO KOSHIKAWA, KENSEI YAHATA, HISASHI MAKINO, TETSUYA NAGAE, YURIKO FUJINAGA, HIDEKI YOKOI, TETSURO YOSHIOKA, AKIHIRO YOSHIMOTO, ISSEI TANAKA, and KAZUWA NAKAO

Department of Medicine and Clinical Science, Kyoto University Graduate School of Medicine, Kyoto, Japan.

Abstract. Dynamic recovery of glomerular structure occurs after severe glomerular damage in anti-Thy-1 glomerulonephritis (Thy-1 GN), but its mechanism remains to be investigated. To identify candidate genes possibly involved in glomerular reconstruction, screening was performed for genes that are specifically expressed by podocytes and are upregulated in glomeruli of Thy-1 GN. Among them, cysteine-rich protein 61 (Cyr61 or CCN1), a soluble angiogenic protein belonging to the CCN family, was identified. By Northern blot analysis, Cyr61 mRNA was markedly upregulated in glomeruli of Thy-1 GN from day 3 through day 7, when mesangial cell migration was most prominent. By *in situ* hybridization and immunohistochemistry, Cyr61 mRNA and protein were expressed by proximal straight tubules and afferent and efferent arterioles in normal rat kidneys and were intensely upregulated at podocytes in Thy-1 GN. Platelet-derived growth factor–BB (PDGF-BB) and transforming growth factor–β1 (TGF-β1), of which the gene expression in the glomeruli of Thy-1 GN was upregulated in similar time course as Cyr61, induced Cyr61 mRNA expression in cultured podocytes. Furthermore, supernatant of Cyr61-overexpressing cells inhibited PDGF-induced mesangial cell migration. In conclusion, it is shown that Cyr61 is strongly upregulated at podocytes in Thy-1 GN possibly by PDGF and TGF-β. Cyr61 may be involved in glomerular remodeling as a factor secreted from podocytes to inhibit mesangial cell migration.

The glomeruli of the kidney seem to possess an ability to repair their own structure, because resolution of glomerular sclerotic lesions occurs in diabetic patients after pancreas transplantation (1). Rat anti-Thy-1 glomerulonephritis (Thy-1 GN) is one of the best-studied reversible models of glomerulonephropathy (2–5). In this model, mesangiolysis leads to severe destruction of glomerular structure, characterized by so-called "ballooning lesions." Glomerular reconstruction begins with migration of mesangial cells from vascular poles and angiogenesis by immature endothelial cells (2,3). During the course of glomerular remodeling, various soluble factors have been identified to be expressed by mesangial cells, such as platelet-derived growth factor (PDGF), basic fibroblast growth factor, and endothelin (5). However, most of them enhance mesangial cell proliferation and potentially exacerbate glomerulonephritis. On the other hand, vascular endothelial growth factor, secreted by mesangial cells, podocytes, and infiltrating leukocytes, enhances the recovery by stimulating endothelial cell proliferation (6,7). Other soluble factors may also be involved in this complex process.

A characteristic feature of Thy-1 GN is that podocytes are kept almost intact throughout the course. Preceding minor podocyte injury to this model leads to irreversible mesangial alteration (8), demonstrating the importance of podocytes for the glomerular recovery in this model. These findings suggest that podocytes contribute to maintenance and recovery of the glomerular structure by counteracting the hydrostatic force on the glomerular filtration barrier mechanically. Furthermore, it is also possible that podocytes may regulate mesangial migration, proliferation, or matrix accumulation by secreting undetermined factors and that these factors might play a role in glomerular remodeling during Thy-1 GN. Therefore, to identify new candidate genes possibly involved in the reconstruction of damaged glomeruli, we screened for genes whose expressions are podocyte-specific and are upregulated in the glomeruli of Thy-1 GN. Using the suppressive subtractive hybridization method, we identified several such genes, one of which was cysteine-rich protein 61 (Cyr61 or CCN1).

Cyr61 is a secreted, heparin-binding extracellular matrix-binding protein belonging to the CCN family, which also includes connective tissue growth factor (CTGF or CCN2), nephroblastoma overexpressed (Nov or CCN3), and Wnt-induced secreted proteins-1, -2, and -3 (WISP-1, 2, 3 or CCN-4, 5, 6, respectively) (9–11).

Received October 11, 2002. Accepted January 23, 2003.
Correspondence to Dr. Kiyoshi Mori, Department of Medicine and Clinical Science, Kyoto University Graduate School of Medicine, 54 Shogoin Kawahara-cho, Sakyo-ku, Kyoto 606-8507, Japan. Phone: 81-75-751-4286; Fax: 81-75-771-9452; E-mail: keyem@kuhp.kyoto-u.ac.jp
1046-6673/1405-1154
Journal of the American Society of Nephrology

DOI: 10.1097/01.ASN.0000060576.61218.3D

Cyr61 stimulates migration and proliferation of vascular endothelial cells and fibroblasts in culture and induces neovascularization in rat corneas (12–14). To date, Cyr61 expression or its role in the kidney remains unknown.

In this study, we revealed that Cyr61 is upregulated in the glomeruli of Thy-1 GN. We investigated the sites of Cyr61 expression in normal rat kidneys and in Thy-1 GN and its regulation in cultured podocytes. Furthermore, we studied the effect of Cyr61 on mesangial cell migration and proliferation. Our data suggest that Cyr61 expressed in podocytes may be involved in glomerular remodeling during Thy-1 GN.

Materials and Methods

Cell Culture

An immortalized mouse podocyte cell line, MPC5, was a kind gift from Dr. Peter Mundel, Albert Einstein College of Medicine, Bronx, New York (15). These cells proliferate when cultured with 10 U/ml murine interferon-γ (INF-γ; Life Technologies, Gaithersburg, MD) at 33°C (permissive condition), whereas they halt growing and begin to differentiate to express podocyte-specific genes such as synaptopodin when cultured without INF-γ at 37°C (nonpermissive condition). Podocytes were cultured with RPMI 1640 medium (Nihonseiyaku, Tokyo, Japan) supplemented with 10% fetal calf serum (FCS; Cansera International, Ontario, Canada), 10 U/ml penicillin, and 10 μg/ml streptomycin (ICN Biomedicals, Costa Mesa, CA) on dishes coated with 100 μg/ml type I collagen (Cellgen IPC-03; KOKEN, Tokyo, Japan). Before each experiment, cells were differentiated under nonpermissive condition on type I collagen-coated dishes for 2 wk without passage and cultured with RPMI 1640 containing 0.5% bovine serum albumin (BSA; Sigma, St. Louis, MO) for 24 h, until stimulation with 5 ng/ml human transforming growth factor–β1 (TGF-β1) or 10 ng/ml human PDGF-BB (R&D Systems, Minneapolis, MN). Cells were used between passages 15 and 20 (15).

Mesangial cells were established from glomeruli of 4 to 6-wk-old Sprague-Dawley rats as described previously (16). Mesangial cells were cultured with Dulbecco Modified Eagle Medium (DMEM; Invitrogen, Carlsbad, CA) with 10% FCS and antibiotics and used between passages 7 and 10.

Generation of Podocyte-Specific cDNA Library

To generate a cDNA library of podocyte-specific genes (PSG), we applied the suppressive subtractive hybridization procedure between cDNA pools derived from differentiated mouse podocytes and from C57BL/6 mouse whole kidney using PCR-Select cDNA Subtraction Kit (Clontech, Palo Alto, CA). Total RNA from each sample was extracted by TRIZOL Reagent (Invitrogen), and poly(A)$^+$ mRNA was isolated using PolyATtract mRNA Isolation System IV (Promega, Madison, WI). To confirm podocyte-specific expression of each cDNA, we performed differential screening by reverse Northern blot analysis. cDNA fragments were blotted in quadruplicate on four sets of nylon membranes (GeneScreen Plus; NEN Life Science Products, Boston, MA) and hybridized with four different ^{32}P-labaled cDNA pools using PCR-Select Differential Screening Kit (Clontech): podocyte (Pod) subtracted with whole kidney (WK) (Pod − WK); WK − Pod; Pod unsubtracted; and WK unsubtracted. The blots were exposed to BAS-III imaging plate (Fuji, Tokyo, Japan).

Generation of Anti-Thy-1 Glomerulonephritis

All animal experiments were conducted in accordance with our institutional guidelines for animal research. Mouse monoclonal antibody against rat Thy-1 (CD90) antigen (CL005A; Cedarlane, Ontario, Canada) (17) was washed and concentrated in phosphate-buffered saline (PBS) using dialysis membrane (Slide-A-Lyser; Pierce, Rockford, IL) for 16 h at 4°C. Glomerulonephritis was induced in Wistar rats (150 to 200 g) by intravenous administration of 1.5 mg/kg anti-Thy-1 antibody diluted in 0.7 ml PBS from tail vein. The rats were killed after antibody administration for histologic examination of kidney tissues and for isolation of glomeruli to extract total RNA. For light microscopic study, kidney tissues were fixed with Dubosq-Brazil solution for 12 h at 4°C and embedded in paraffin.

Library Screening for Genes Upregulated in Anti-Thy-1 Glomerulonephritis and Nucleotide Sequencing

PSG were blotted identically on four different nylon membranes (GeneScreen Plus) and hybridized with four different ^{32}P-labeled cDNA pools derived from glomeruli of Thy-1 GN at days 0, 1, 3, and 5 using PCR-Select Differential Screening Kit. In this screening, mouse cDNAs blotted on membranes were hybridized with rat cDNA probes, because we expected that most, if not all, cDNAs have enough sequence homologies for cross-hybridization. The nucleotide sequences of cDNAs whose expression levels were increased in Thy-1 GN were determined by BigDye Terminator (Applied Biosystems, Foster City, CA) and ABI PRISM 310 Genetic Analyzer (Applied Biosystems).

Northern Blot Analyses

Northern blot analysis was performed as described (18). In brief, total RNA (30 μg in each lane) was electrophoresed on 1.0% agarose gels and transferred to nylon membranes (GeneScreen Plus). The cDNA fragments of rat Cyr61 (see below), rat CTGF (nucleotides 1221 to 1803, GenBank accession number AF120275, generated by reverse transcription [RT]-PCR) (19), rat PDGF-B (nucleotides 38 to 666, GenBank accession number Z14117, generated by RT-PCR) (20), and human glyceraldehyde-3-phosphate dehydrogenase (GAPDH, Clontech) were used as probes. The membranes were hybridized with [^{32}P]dCTP-labeled probes, and the blots were exposed to BAS-III imaging plate. The amount of RNA loaded in each lane was normalized for 28S ribosomal RNA or GAPDH.

In Situ Hybridization Analyses

Rat Cyr61 cDNA fragment was cloned by RT-PCR with sense primer 5'-tgcgcgccacaatgagctccagca-3' and antisense primer 5'-cccaggagacctttagtccctgaa-3' (nucleotides 175 to 1337, GenBank accession number AF218568) (21) using total RNA from Wistar rat kidneys. Sense and antisense [^{35}S]CTP-labeled cRNAs were generated from the rat Cyr61 cDNA ligated in pGEM-T easy vector (Promega) using T7 and SP6 RNA polymerases (Promega). *In situ* hybridization analysis was performed as described previously (22). In brief, 10-μm cryosections of rat kidneys were mounted on poly-L-lysine-coated slides, fixed with paraformaldehyde, acetylated, and hybridized with the cRNA probes. Slides were washed, dehydrated, and apposed to Hyperfilm β-max films (Amersham, Buckinghamshire, UK) for 10 d or dipped into autoradiographic emulsion (NTB-2, Eastman Kodak, Rochester, NY) and exposed for 6 wk and counterstained with hematoxylin and eosin.

Immunohistochemical Analyses

Deparaffinized 3-μm kidney sections were treated with microwave heating (5 min twice in 10 mM citrate buffer, pH 7.4). Endogenous peroxidase was blocked by incubation with 3% hydrogen peroxide for 15 min at room temperature. Goat anti-human Cyr61 antibody (sc-

8561; Santa Cruz Biotechnology, Santa Cruz, CA) was diluted 1:300 in PBS containing 1% BSA (1% BSA/PBS) and was incubated for 1 h at room temperature. After washes with 1% BSA/PBS, the sections were incubated with biotinylated secondary antibody (sc-2347, biotin-conjugated bovine anti-goat Ig; Santa Cruz Biotechnology) diluted 1:100 in 1% BSA/PBS for 30 min at room temperature. The sections were further processed with avidin-biotin-peroxidase complex kit (Vector, Burlingame, CA) and 3,3'-diaminobenzidine tetrahydrochloride (Kanto Chemical, Tokyo, Japan), and counterstained with hematoxylin and coverslipped. Nonimmune goat serum was used as negative control. To further confirm the specificity of the signals, anti-Cyr61 antibody was preincubated overnight at 4°C with blocking peptide (sc-8561 P, Santa Cruz Biotechnology) at the five-times higher concentration (weight/volume) than the antibody concentration before incubation with the sections.

Overexpression of Cyr61 and Western Blot Analyses

COS-7 cells were cultured with DMEM supplemented with 10% FCS and antibiotics. Full-length mouse Cyr61 cDNA was generated by RT-PCR using total RNA from C57BL/6 mouse kidneys and the following primers: sense 5'-tgcgcgccacaatgagctccagca-3' and antisense 5'-ttagtccctgaacttgtggatgtc-3' (nucleotides 179 to 1329, GenBank accession number M32490) (23). The Cyr61 cDNA was first TA-cloned into pGEM-T easy vector and transferred into *Eco*RI restriction site of expression vector pCXN2, a derivative of pCAGGS (24). COS-7 cells were transfected with Cyr61-pCXN2 or mock-pCXN2 cDNA using Lipofectamine Plus Reagent (Invitrogen). Media were changed 3 h after transfection, harvested 69 h later, and kept −20°C until they were used for functional assay (see below). At 72 h after transfection, cells were lysed on ice in solution that contained 20 mM Tris-HCl (pH 7.5), 12 mM-glycerophosphate, 0.1 M ethyleneglycol-bis(-aminoethyl ether)-N,N'-tetraacetic acid, 1 mM pyrophosphate, 5 mM NaF, 5 mg/ml aprotinin, 2 mM dithiothreitol, 1 mM phenylmethylsulfonyl fluoride, 1% Triton X-100 (Nacalai Tesque, Kyoto, Japan), and 1 mM sodium orthovanadate (Sigma) (25). The lysate was centrifuged at 15,000 rpm for 20 min at 4°C, and the supernatant was mixed with Laemmli sample buffer. Samples were separated by 12.5% SDS-PAGE in reducing conditions and electrophoretically transferred onto Immobilon polyvinylidine difluoride filters (Millipore, Bedford, MA). The filters were incubated with anti-Cyr61 antibody diltuted 1:1000 in Block Ace (Snow Brand Milk Products, Sapporo, Japan) for 2 h at room temperature and were developed with horseradish peroxidase (HRP)–conjugated donkey anti-goat IgG (sc-2020, Santa Cruz Biotechnology) and chemiluminescence kit (ECL, Amersham).

Cell Migration Assay

Migration of mesangial cells was analyzed by modified Boyden chamber method using 96-well chemotaxis chambers (AB96, Neuro Probe, Gaithersburg, MD) (26). Polycarbonate filters (8-μm pore size, PFD8, Neuro Probe) coated with 20 ng/ml poly-L-lysine (Sigma) for 24 h at 25°C were placed in the middle of the chambers, and the number of cells that moved from the upper chambers to the lower chambers was counted. Mesangial cells suspended in supernatant of mock-transfected COS-7 cells (1×10^5 cells/100 μl per well) were placed in the top chambers. In the lower chambers, 30-μl supernatant of Cyr61-transfected or mock-transfected COS-7 cells supplemented with or without PDGF-BB was placed. The chambers were incubated in humidified air with 5% CO_2 for 3 h at 37°C. The cells remaining on the upper surfaces of the filters were scraped off, and the cells that had migrated to the lower surfaces were fixed in methanol and stained with 0.5% Coomassie Brilliant Blue R 250 (Nacalai Tesque) in 50% methanol, 40% water, and 10% acetic acid. For each well, 5 high-power field photographs (magnification, ×400) were taken to calculate the mean number of cells migrated per high-power field.

Cell Proliferation Assay

Mesangial cells were plated on 24-well plates at 2×10^4 cells/well, grown for 24 h, and incubated with DMEM containing 0.2% FCS for the following 24 h. Cells were then treated with media containing supernatant of Cyr61-transfected or mock-transfected COS-7 cells diluted 1:1 by fresh DMEM containing 10% FCS, with or without 10 ng/ml PDGF-BB. [^{3}H]-thymidine (3 μCi/ml, Amersham) was added simultaneously with the above-described media. After 48 h of incubation, cells were washed with PBS and fixed with 10% TCA (Nacalai Tesque). DNA was dissolved in 0.25 N NaOH, and incorporated thymidine was counted in liquid scintillation counter (Aloka, Tokyo, Japan) as described previously (25).

Statistical Analyses

Results are given as means ± SEM. Mann-Whitney U test was used to compare unpaired two-group means. The differences were evaluated with a Stat View software package (Abacus Concepts Inc., Berkeley, CA), and those with $P < 0.05$ were considered statistically significant.

Results

Construction of Podocyte-Specific cDNA Library

To construct a cDNA library of PSG, subtraction of cultured mouse Pod cDNA pool with mouse WK cDNA pool was performed (Pod − WK), and each of 1500 subtracted cDNA clones was placed in grids to make four identical sets of PSG array. To confirm specific expression of PSG, we performed reverse Northern blot analyses using ^{32}P-labeled Pod − WK, WK − Pod, Pod, and WK cDNA probes, respectively. Representative results showed that thrombospondin-1 and ceruloplasmin are expressed intensely and specifically in cultured podocytes, whereas fibronectin is expressed abundantly in whole kidney (Figure 1). By this screening, 150 clones of highly podocyte-specific genes were isolated.

Histologic Examination of Anti-Thy-1 Glomerulonephritis

We next examined the time course of histologic alteration during Thy-1 GN with light microscopy (data not shown). In the present study, we used anti-Thy-1 antibody at the concentration sufficient to cause almost complete elimination of mesangial cells at day 1. At day 3 of Thy-1 GN, most of mesangial cells were located at vascular poles, suggesting that mesangial cells were migrating into glomerular tufts (2). They reached the periphery of most glomerular tufts at day 7. Glomerular microaneurysms appeared at day 3, progressing to ballooning lesion at day 5, which indicated that severe destruction of the capillary tufts occurred. At day 10, microaneurysms were observed in only few glomeruli. At day 21, mesangial cell and matrix accumulation were still seen, but they subsided at day 28.

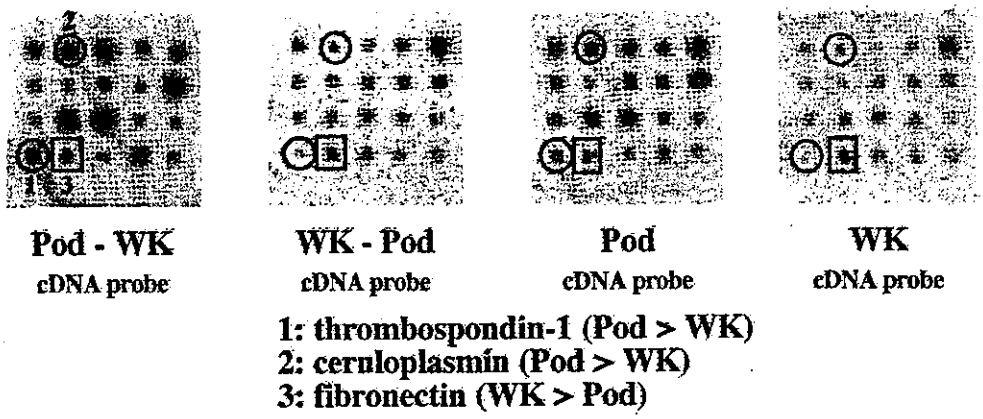

Figure 1. Screening for genes specifically expressed in cultured podocytes (Pod). Pod-derived cDNAs subtracted with whole kidney (WK)–derived cDNAs (Pod − WK) were blotted in quadruplicate and hybridized with four kinds of cDNAs obtained from Pod − WK, WK − Pod, Pod, and WK, respectively. Clones 1 and 2 were expressed more intensely in Pod than in WK, while expression of clone 3 was more abundant in WK.

Identification of Cyr61 as PSG Upregulated in the Glomeruli of Anti-Thy-1 Glomerulonephritis

To isolate PSG possibly involved in glomerular reconstruction, we examined which PSG were upregulated in the glomeruli of Thy-1 GN. We carried out second set of reverse Northern blot analyses by radiolabeling glomerular cDNA of Thy-1 GN at days 0, 1, 3, and 5. Of 150 PSG clones, we identified 40 to be upregulated, and we determined their nucleotide sequences. One of them was a cDNA fragment of Cyr61 (nucleotides 1290 to 1568, GenBank accession number M32490) (23), which is known as a soluble angiogenic protein associated with extracellular matrix (9,10).

Cyr61 Expression in Normal Kidney and in Anti-Thy-1 Glomerulonephritis

In Thy-1 GN, glomerular gene expression of Cyr61 was low at day 0, increased significantly from day 1 through day 7, reaching the peak at day 5 by 4.5-fold, and gradually decreased toward day 10 by Northern blot analysis (Figure 2). The gene expression of CTGF, another member of the CCN family, was similar to Cyr61, peaking at day 3. We also examined the gene expression of growth factors that have been implicated in Thy-1 GN (5) and found that gene expression of PDGF-B and TGF-β1 in glomeruli was also induced maximally around days 3 to 5.

To examine the location of Cyr61 gene expression in normal kidney and in Thy-1 GN, *in situ* hybridization was performed with ^{35}S-labeled cRNA probe (Figure 3). At autoradiograph, moderate hybridizing signals were observed in outer stripe of outer medulla in normal kidney. At day 5 of Thy-1 GN, strong signals were seen in dot pattern in cortex. At photomicrograph, these signals in Thy-1 GN were observed intensely in glomeruli, consistently with the findings by Northern blot analysis (Figure 2).

Precise sites of Cyr61 expression were further studied by immunohistochemistry with antibody against Cyr61 (Figure 4). In normal kidney, Cyr61 protein was expressed in outer stripe of outer medulla, which corresponded to brush border membrane-positive proximal straight tubules (S3 segment). At high-power field, intense expression of Cyr61 protein was also

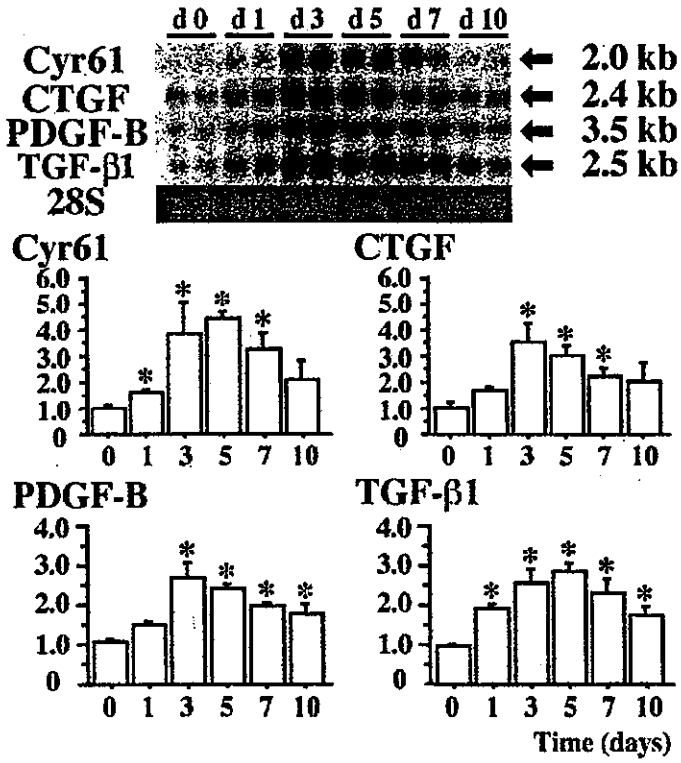

Figure 2. Gene expression of Cyr61, connective tissue growth factor (CTGF), platelet-derived growth factor-B (PDGF-B), and transforming growth factor–β1 (TGF-β1) in glomeruli of anti-Thy-1 glomerulonephritis. Cyr61, CTGF, PDGF-B and TGF-β1 expressions were all induced maximally around days 3 to 5 by Northern blot analysis. The graphs on the bottom show relative gene expression level of each gene normalized for ethidium bromide staining intensity of 28S ribosomal RNA. The level at day 0 was arbitrarily defined as 1. * $P < 0.05$ as compared with day 0; $n = 3$.

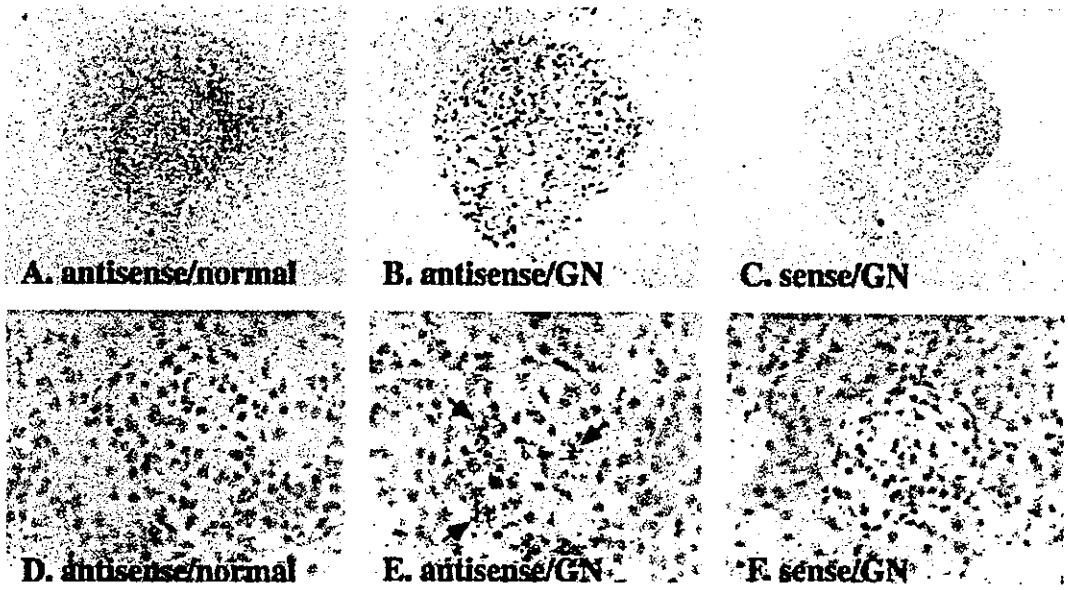

Figure 3. Localization of Cyr61 gene expression in normal kidney and in anti-Thy-1 glomerulonephritis by *in situ* hybridization. Antisense (A, B, D, and E) or sense (C and F) Cyr61 cRNA probe was hybridized with sections from normal kidney (A and D) and Thy-1 GN (B, C, E, and F), and autoradiograph (A through C, ×4) and photomicrograph with counterstaining by hematoxylin and eosin (D through F, ×400) were carried out. In normal kidney, Cyr61 gene was expressed predominantly in outer stripe of outer medulla (A); in Thy-1 GN at day 5, it was induced markedly in glomeruli (B and E, arrow). No specific signals were seen in sections hybridized with the sense probe (C and F).

observed in some of afferent and efferent arterioles in normal kidney, but the protein was not expressed in larger vessels. At day 5 of Thy-1 GN, Cyr61 expression was also detected in glomeruli. The signals were observed on outer surfaces of glomerular basement membrane (GBM), which appeared to be podocytes. Anti-Cyr61 antibody specifically recognized Cyr61 protein (40 kD) expressed in COS-7 cells by Western blot analysis. Specificity of the antibody binding in immunohistochemistry was further confirmed by disappearance of the signals when the antibody was preabsorbed with blocking peptide (data not shown) or when nonimmune serum was used as primary antibody. The expression of Cyr61 mRNA and protein in glomeruli and podocytes increased in Thy-1 GN, whereas expression in tubules and arterioles did not seem to change in Thy-1 GN.

Cyr61 Induction by PDGF-BB and TGF-β1 in Cultured Podocytes

To explore the regulatory mechanism of Cyr61 expression in podocytes, cultured podocytes were treated with PDGF-BB or TGF-β1, because we found that PDGF-B, TGF-β1, and Cyr61 genes were coordinately upregulated in Thy-1 GN. Treatment of podocytes with 10 ng/ml PDGF-BB upregulated Cyr61 gene expression significantly at 10 min by 1.2-fold and at 24 h by 1.5-fold (Figure 5). Addition of 5 ng/ml TGF-β1 to podocytes induced Cyr61 expression significantly at 1 h by 2.2-fold and 24 h by 2.1-fold (Figure 6). We also observed that PDGF-BB and TGF-β1 caused upregulation of CTGF gene expression in podocytes significantly at 10 min to 24 h and at 1 to 24 h, respectively.

Inhibition of PDGF-Induced Mesangial Cell Migration by Supernatant of Cyr61-Overexpressing Cells

To examine the functional role of Cyr61 upregulation in podocytes during Thy-1GN, migration of mesangial cells in supernatant of Cyr61-transfected or mock-transfected COS-7 cells was studied using modified Boyden chambers (Figure 7). In the absence of PDGF-BB, supernatant of Cyr61-transfected COS-7 cells had no significant effect on mesangial cell migration compared with that of mock-transfected COS-7 cells. With addition of 10 ng/ml PDGF-BB, cell migration in mock-transfected supernatant was enhanced by 2.4-fold. On the other hand, conditioned media from Cyr61-overexpressing cells significantly suppressed PDGF-induced mesangial cell migration by 24%.

No Effects of Supernatant of Cyr61-Overexpressing Cells on Mesangial Cell Proliferation

We further examined whether culture media from Cyr61-transfected cells affect proliferation of mesangial cells (Figure 8). PDGF-BB significantly increased mesangial cell numbers by twofold after 48 h, but addition of supernatant of Cyr61-transfceted cells had no significant effects on cell numbers both in the absence and presence of PDGF and on PDGF-induced DNA synthesis.

Discussion

In the present study, we generated a podocyte-specific cDNA library and investigated the expression levels of the cDNAs during Thy-1 GN, a reversible model of glomerular disease, and identified that gene expression of soluble angiogenic factor Cyr61 was highly induced in the glomeruli of

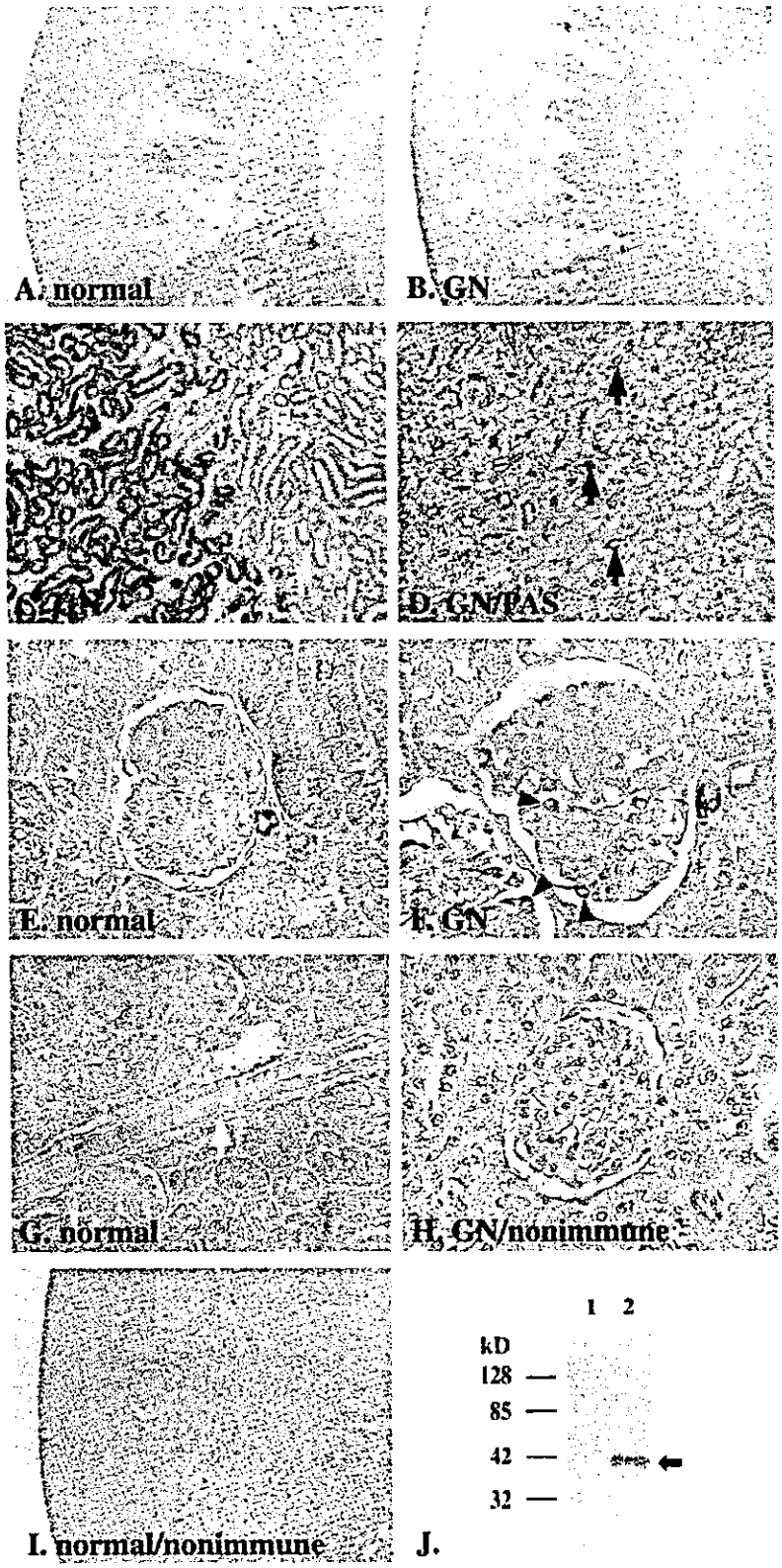

Figure 4. Immunohistochemical analyses of Cyr61 protein expression in normal kidney and in anti-Thy-1 glomerulonephritis. In normal kidney (A) and in Thy-1 GN at day 5 (B), Cyr61 protein was expressed in outer stripe of outer medulla. The analysis of high-power field at the border between outer and inner stripes (C and D) revealed that the signals were confined to proximal straight tubules (C) with brush border membranes, which were visualized as pink by periodic acid-Schiff (PAS) staining in the adjacent section (D, black arrow). Cyr61 protein was also expressed intensely in some, but not all, afferent and efferent arterioles in normal kidney (E). The protein was not expressed in larger vessels such as interlobular arteries (G, white arrow). In Thy-1 GN at day 5, Cyr61 expression was also seen in podocytes (F, arrowhead), which were present outside of glomerular basement membrane. Incubation of sections with nonimmune serum as primary antibody gave no signals in proximal straight tubules (I), arterioles or podocytes in Thy-1 GN (H). By Western blot analysis (J), anti-Cyr61 antibody specifically recognized a 40-kD protein in lysate of Cyr61-transfected COS-7 cells (lane 2, arrow), but not in that of mock-transfected cells (lane 1). Magnifications: ×40 in A, B, and I; ×200 in C, D, and G; ×400 in E, F, and H.

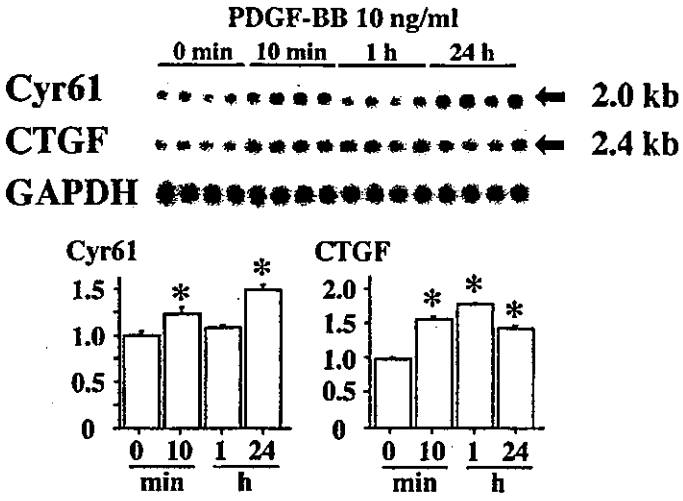

Figure 5. PDGF-BB-induced Cyr61 and CTGF gene expression in cultured podocytes. PDGF-BB was added to podocytes and the time course of Cyr61 and CTGF gene expression was examined by Northern blot analyses. The graphs on the bottom show relative gene expression level of each gene normalized for GAPDH expression. The level in untreated podocytes (control) was arbitrarily defined as 1. * $P < 0.05$ as compared with control; $n = 4$.

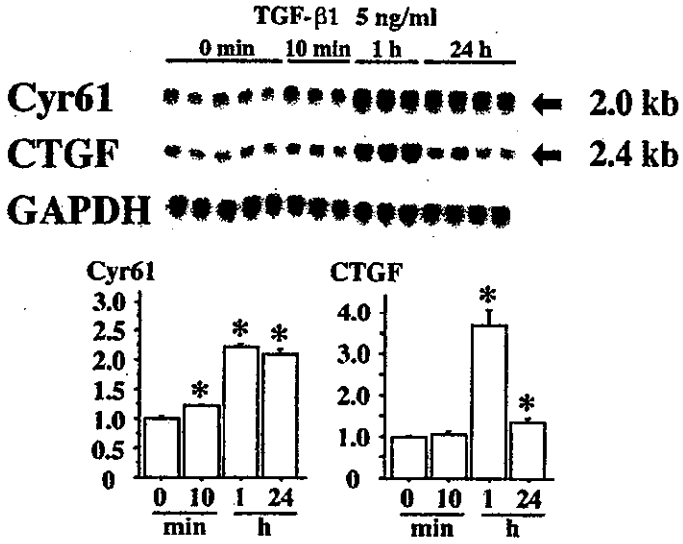

Figure 6. TGF-β1–induced Cyr61 and CTGF gene expression in cultured podocytes. * $P < 0.05$ as compared with control; $n = 3$ to 5.

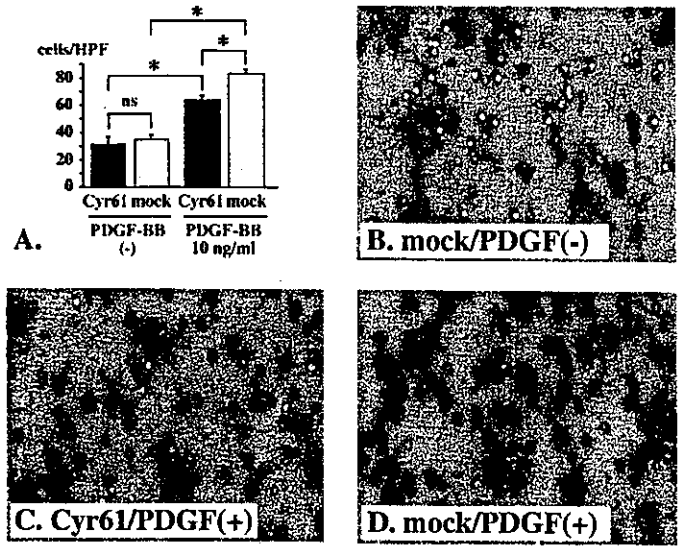

Figure 7. Effects of culture media of Cyr61-overexpressing cells on PDGF-BB-induced mesangial cell migration. Mesangial cells plated in modified Boyden chambers were incubated for 3 h with supernatant of Cyr61-transfected or mock-transfected COS-7 cells, which was supplemented with or without PDGF-BB. In the absence of PDGF-BB, supernatant of Cyr61-transfected COS-7 cells had no effects on cell migration compared with that of mock-transfected COS-7 cells (A). In culture media from mock-transfected cells, addition of 10 ng/ml PDGF-BB significantly increased mesangial cell migration (B and D). Supernatant of Cyr61-overexpressing cells significantly suppressed the chemotaxis in the presence of PDGF-BB (C and D). * $P < 0.05$; ns, not statistically significant; HPF, high-power field; $n = 4$ to 8. Magnification, ×400 in B through D.

Thy-1 GN. We revealed for the first time, at least to our knowledge, that Cyr61 gene and protein expression was specifically induced in podocytes in Thy-1 GN and that physiologic sites of Cyr61 expression were proximal straight tubules and afferent and efferent arterioles. PDGF-B and TGF-β1 were upregulated in similar time course as Cyr61 in Thy-1 GN, and they induced Cyr61 gene expression in cultured podocytes, suggesting that they are inducers of podocyte Cyr61 expression *in vivo*. Furthermore, culture media of Cyr61-transfected cells inhibited mesangial cell migration induced by PDGF-BB, suggesting that Cyr61 may be involved in glomerular remodeling in Thy-1 GN.

In glomeruli of Thy-1 GN, Cyr61 gene expression was markedly upregulated from day 3 through day 7, when mesangial cell migration was most active, as shown by our histologic analysis, which was consistent with previous reports (2–5). Furthermore, neovascularization, characterized with immature endothelial cell proliferation, is also reported to take place in a period involving days 3 to 7 (2,17). Cyr61 exerts various actions through interaction with cell surface integrin heterodimer complexes (13,27–29). Cyr61 induces endothelial cell migration through integrin $\alpha_v\beta_3$ and stimulates neovascularization in rat cornea (12). In fibroblasts, Cyr61 induces cell migration through $\alpha_v\beta_5$ and proliferation through $\alpha_v\beta_3$ (13). Mesangial cells also express $\alpha_v\beta_3$ and $\alpha_v\beta_5$ integrins (30); therefore, an angiogenic factor Cyr61, which has high affinity to extracellular matrix (31), may be secreted by podocytes, bound to GBM, and act upon endothelial and mesangial cells to modulate migration and proliferation during remodeling of glomerular structure in Thy-1 GN.

A regulatory role of podocytes on mesangial cells has been implied by recent studies. One study showed that minor podocyte injury with puromycin preceding Thy-1 GN induction results in irreversible mesangial lesions (8). Another report demonstrated that mice deficient of podocyte-specific mole-

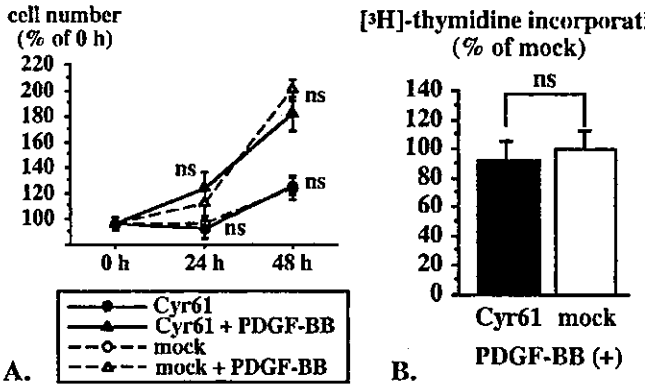

Figure 8. Effects of culture media of Cyr61-overexpressing cells on mesangial cell proliferation. Mesangial cells were incubated with media containing supernatant of Cyr61-transfected or mock-transfected COS-7 cells, together with or without 10 ng/ml PDGF-BB. The cell numbers after 24 h and 48 h were not significantly different between the treatments with Cyr61-conditioned and control media, both in the absence and presence of PDGF-BB (A). Supernatant of Cyr61-overexpressing cells also did not significantly affect PDGF-BB-induced mitogenesis as judged by [^{3}H]-thymidine incorporation after 48 h (B). ns, not statistically significant; n = 6 to 12.

cule CD2-associated protein exhibit mesangial cell proliferation and mesangial matrix expansion (32). These findings seem to raise a possibility that factors secreted from podocytes may regulate mesangial cell activity. In the present study, we found that supernatant of cells transfected with Cyr61, a candidate for such podocyte-derived factors, inhibited PDGF-BB-induced mesangial cell migration, implying that podocytes may suppress migratory activity of mesangial cells when mesangial cells reach the periphery of glomerular tufts, that is GBM, and may help the cessation of glomerulonephritis. Cyr61 enhances both migration and growth factor-induced proliferation in vascular endothelial cells and fibroblasts (12–14). However, here we show that, in mesangial cells, Cyr61-conditioned media inhibited PDGF-BB-induced migration but did not affect PDGF-BB-induced proliferation. The discrepancy may be due to distinct responses in different cells or due to difference in experimental settings: use of culture media of transfected cells *versus* recombinant protein.

Cyr61 protein has been reported to be synthesized by serum-stimulated NIH 3T3 fibroblasts, but it is associated with extracellular matrix and cannot be detected in the conditioned media (31). When we overexpressed Cyr61 in COS-7 cells, Cyr61 protein was detected in the supernatant by Western blot analysis (data not shown), but several possibilities can still be considered concerning the mechanism for migration inhibitory effects of Cyr61. First, Cyr61 may bind directly to mesangial cells and exert its action, presumably through cell surface integrin complexes (see above). Second, Cyr61 might interact with PDGF in the media to interfere with its action, as is the case with CTGF and bone morphogenic protein 4 reported in *Xenopus* (33). Third, Cyr61 may alter secretion of other soluble factors such as extracellular matrix proteins (see below) from COS-7 cells, which have activity to modify mesangial cell migration.

Previous reports showed that Cyr61 is expressed in endothelial and smooth muscle cells in the developing mouse blood vessels (34,35) but only weakly in vessels of normal adult mice and humans (36). In the present study, Cyr61 was expressed in normal afferent and efferent arterioles, in which Cyr61 expression might be upregulated by strong mechanical stretch due to shear stress (37).

Cyr61 and CTGF share structural and functional similarity and belong to the CCN family (9,10), but their tissue distribution (31) and intrarenal localization is clearly different. In normal kidney, the main site of Cyr61 expression was proximal straight tubules. On the contrary, we and others have shown that neither CTGF gene (19,38) nor protein (31,39,40) are expressed in normal proximal tubules. In glomeruli of Thy-1 GN, Cyr61 protein expression was predominantly induced in podocytes, whereas CTGF gene expression is broadly upregulated in podocytes, glomerular parietal epithelial cells, mesangial cells, and periglomerular myofibroblasts (39). The spatial differences of Cyr61 and CTGF transcriptional regulation in physiologic and pathophysiologic conditions suggest that Cyr61 and CTGF play distinct roles *in vivo*. Furthermore, recent studies revealed functional difference between Cyr61 and CTGF; in fibroblasts CTGF upregulates collagen I and fibronectin expression (19,41), whereas Cyr61 does not upregulate fibronectin expression but rather downregulates collagen I expression (42).

In conclusion, we show that Cyr61, which exerts suppressive effects on mesangial cell migration, is strongly upregulated at podocytes in Thy-1 GN during a phase when mesangial cell migration is active. These findings raise a possibility that podocytes may participate in the reconstruction of glomeruli by secreting factors that affect mesangial cell activity. Possible autocrine and paracrine role of Cyr61 not only in podocytes but also in arterioles and tubular cells also must be investigated in future studies.

Acknowledgments

The authors gratefully acknowledge Dr. Peter Mundel (Albert Einstein College of Medicine) for providing mouse podocyte cell line MPC5, Dr. Jun-ichi Miyazaki (Osaka University, Japan) for expression vector pCXN2, Dr. Akira Shimizu (Nippon Medical School, Japan) for technical suggestion to generate Thy-1 GN, and Dr. Takashi Kuwahara (Saiseikai Nakatsu Hospital, Japan) for technical advice for histologic examination. We are also grateful to J. Nakamura and A. Wada for technical assistance, and A. Sonoda and S. Doi for secretarial assistance. This work was supported in part by research grants from the Japanese Ministry of Education, Science, Sports and Culture, the Japanese Ministry of Health and Welfare, Smoking Research Foundation, and "Research for the Future" (RFTF) of Japan Society for the promotion of Science.

References

1. Fioretto P, Steffes MW, Sutherland DE, Goetz FC, Mauer M: Reversal of lesions of diabetic nephropathy after pancreas transplantation. *N Engl J Med* 339: 69–75, 1998
2. Hugo C, Shankland SJ, Bowen-Pope DF, Couser WG, Johnson RJ: Extraglomerular origin of the mesangial cell after injury. A

new role of the juxtaglomerular apparatus. *J Clin Invest* 100: 786–794, 1997
3. Iruela-Arispe L, Gordon K, Hugo C, Duijvestijn AM, Claffey KP, Reilly M, Couser WG, Alpers CE, Johnson RJ: Participation of glomerular endothelial cells in the capillary repair of glomerulonephritis. *Am J Pathol* 147: 1715–1727, 1995
4. Morita T, Churg J: Mesangiolysis. *Kidney Int* 24:1–9, 1983
5. Jefferson JA, Johnson RJ: Experimental mesangial proliferative glomerulonephritis (the anti-Thy-1.1 model). *J Nephrol* 12: 297–307, 1999
6. Ostendorf T, Kunter U, Eitner F, Loos A, Regele H, Kerjaschki D, Henninger DD, Janjic N, Floege J: $VEGF_{165}$ mediates glomerular endothelial repair. *J Clin Invest* 104: 913–923, 1999
7. Masuda Y, Shimizu A, Mori T, Ishiwata T, Kitamura H, Ohashi R, Ishizaki M, Asano G, Sugisaki Y, Yamanaka N: Vascular endothelial growth factor enhances glomerular capillary repair and accelerates resolution of experimentally induced glomerulonephritis. *Am J Pathol* 159: 599–608, 2001
8. Morioka Y, Koike H, Ikezumi Y, Ito Y, Oyanagi A, Gejyo F, Shimizu F, Kawachi H: Podocyte injuries exacerbate mesangial proliferative glomerulonephritis. *Kidney Int* 60: 2192–2204, 2001
9. Brigstock DR: The connective tissue growth factor/cysteine-rich 61/nephroblastoma overexpressed (CCN) family. *Endocr Rev* 20: 189–206, 1999
10. Lau LF, Lam SC: The CCN family of angiogenic regulators: The integrin connection. *Exp Cell Res* 248:44–57, 1999
11. Proposal for a unified CCN nomenclature. *Mol Pathol* 54: 108, 2001
12. Babic AM, Kireeva ML, Kolesnikova TV, Lau LF: CYR61, a product of a growth factor-inducible immediate early gene, promotes angiogenesis and tumor growth: *Proc Natl Acad Sci USA* 95: 6355–6360, 1998
13. Grzeszkiewicz TM, Kirschling DJ, Chen N, Lau LF: CYR61 stimulates human skin fibroblast migration through integrin $\alpha_v\beta_5$ and enhances mitogenesis through integrin $\alpha_v\beta_3$ independent of its carboxyl-terminal domain. *J Biol Chem* 276: 21943–21950, 2001
14. Kireeva ML, Mo FE, Yang GP, Lau LF: Cyr61, a product of a growth factor-inducible immediate-early gene, promotes cell proliferation, migration, and adhesion. *Mol Cell Biol* 16: 1326–1334, 1996
15. Mundel P, Reiser J, Zuniga Mejia Borja A, Pavenstadt H, Davidson GR, Kriz W, Zeller R: Rearrangements of the cytoskeleton and cell contacts induce process formation during differentiation of conditionally immortalized mouse podocyte cell lines. *Exp Cell Res* 236: 248–258, 1997
16. Ishibashi R, Tanaka I, Kotani M, Muro S, Goto M, Sugawara A, Mukoyama M, Sugimoto Y, Ichikawa A, Narumiya S, Nakao K: Roles of prostaglandin E receptors in mesangial cells under high-glucose conditions. *Kidney Int* 56: 589–600, 1999
17. Shimizu A, Masuda Y, Kitamura H, Ishizaki M, Sugisaki Y, Yamanaka N: Recovery of damaged glomerular capillary network with endothelial cell apoptosis in experimental proliferative glomerulonephritis. *Nephron* 79: 206–214, 1998
18. Makino H, Tanaka I, Mukoyama M, Sugawara A, Mori K, Muro S, Suganami T, Yahata K, Ishibashi R, Ohuchida S, Maruyama T, Narumiya S, Nakao K: Prevention of diabetic nephropathy in rats by prostaglandin E receptor EP1-selective antagonist. *J Am Soc Nephrol* 13: 1757–1765, 2002
19. Yokoi H, Mukoyama M, Sugawara A, Mori K, Nagae T, Makino H, Suganami T, Yahata K, Fujinaga Y, Tanaka I, Nakao K: Role of connective tissue growth factor in fibronectin expression and tubulointerstitial fibrosis. *Am J Physiol Renal Physiol* 282: F933–F942, 2002
20. Herren B, Weyer KA, Rouge M, Lotscher P, Pech M: Conservation in sequence and affinity of human and rodent PDGF ligands and receptors. *Biochim Biophys Acta* 1173: 294–302, 1993
21. Albrecht C, von Der Kammer H, Mayhaus M, Klaudiny J, Schweizer M, Nitsch RM: Muscarinic acetylcholine receptors induce the expression of the immediate early growth regulatory gene CYR61. *J Biol Chem* 275: 28929–28936, 2000
22. Mori K, Ogawa Y, Ebihara K, Tamura N, Tashiro K, Kuwahara T, Mukoyama M, Sugawara A, Ozaki S, Tanaka I, Nakao K: Isolation and characterization of CA XIV, a novel membrane-bound carbonic anhydrase from mouse kidney. *J Biol Chem* 274: 15701–15705, 1999
23. Latinkic BV, O'Brien TP, Lau LF: Promoter function and structure of the growth factor-inducible immediate early gene *cyr61*. *Nucleic Acids Res* 19: 3261–3267, 1991
24. Niwa H, Yamamura K, Miyazaki J: Efficient selection for high-expression transfectants with a novel eukaryotic vector. *Gene* 108: 193–199, 1991
25. Suganami T, Mukoyama M, Sugawara A, Mori K, Nagae T, Kasahara M, Yahata K, Makino H, Fujinaga Y, Ogawa Y, Tanaka I, Nakao K: Overexpression of brain natriuretic peptide in mice ameliorates immune-mediated renal injury. *J Am Soc Nephrol* 12: 2652–2663, 2001
26. Kohno M, Yasunari K, Minami M, Kano H, Maeda K, Mandal AK, Inoki K, Haneda M, Yoshikawa J: Regulation of rat mesangial cell migration by platelet-derived growth factor, angiotensin II, and adrenomedullin. *J Am Soc Nephrol* 10: 2495–2502, 1999
27. Kireeva ML, Lam SC, Lau LF: Adhesion of human umbilical vein endothelial cells to the immediate-early gene product Cyr61 is mediated through integrin $\alpha_v\beta_3$. *J Biol Chem* 273: 3090–3096, 1998
28. Jedsadayanmata A, Chen CC, Kireeva ML, Lau LF, Lam SC: Activation-dependent adhesion of human platelets to Cyr61 and Fisp12/mouse connective tissue growth factor is mediated through integrin $\alpha_{IIb}\beta_3$. *J Biol Chem* 274: 24321–24327, 1999
29. Chen N, Chen CC, Lau LF: Adhesion of human skin fibroblasts to Cyr61 is mediated through integrin $\alpha_6\beta_1$ and cell surface heparan sulfate proteoglycans. *J Biol Chem* 275: 24953–24961, 2000
30. Hafdi Z, Lesavre P, Tharaux PL, Bessou G, Baruch D, Halbwachs-Mecarelli L: Role of α_v integrins in mesangial cell adhesion to vitronectin and von Willebrand factor. *Kidney Int* 51: 1900–1907, 1997
31. Kireeva ML, Latinkic BV, Kolesnikova TV, Chen CC, Yang GP, Abler AS, Lau LF: Cyr61 and Fisp12 are both ECM-associated signaling molecules: Activities, metabolism, and localization during development. *Exp Cell Res* 233: 63–77, 1997
32. Shih NY, Li J, Karpitskii V, Nguyen A, Dustin ML, Kanagawa O, Miner JH, Shaw AS: Congenital nephrotic syndrome in mice lacking CD2-associated protein. *Science* 286: 312–315, 1999
33. Abreu JG, Ketpura NI, Reversade B, De Robertis EM: Connective-tissue growth factor (CTGF) modulates cell signalling by BMP and TGF-β. *Nat Cell Biol* 4: 599–604, 2002
34. Latinkic BV, Mo FE, Greenspan JA, Copeland NG, Gilbert DJ, Jenkins NA, Ross SR, Lau LF: Promoter function of the angiogenic inducer Cyr61gene in transgenic mice: Tissue specificity, inducibility during wound healing, and role of the serum response element. *Endocrinology* 142: 2549–2557, 2001

35. O'Brien TP, Lau LF: Expression of the growth factor-inducible immediate early gene cyr61 correlates with chondrogenesis during mouse embryonic development. *Cell Growth Differ* 3: 645–654, 1992
36. Hilfiker A, Hilfiker-Kleiner D, Fuchs M, Kaminski K, Lichtenberg A, Rothkotter HJ, Schieffer B, Drexler H: Expression of CYR61, an angiogenic immediate early gene, in arteriosclerosis and its regulation by angiotensin II. *Circulation* 106: 254–260, 2002
37. Tamura I, Rosenbloom J, Macarak E, Chaqour B: Regulation of Cyr61 gene expression by mechanical stretch through multiple signaling pathways. *Am J Physiol Cell Physiol* 281: C1524–1532, 2001
38. Ito Y, Aten J, Bende RJ, Oemar BS, Rabelink TJ, Weening JJ, Goldschmeding R: Expression of connective tissue growth factor in human renal fibrosis. *Kidney Int* 53: 853–861, 1998
39. Ito Y, Goldschmeding R, Bende R, Claessen N, Chand M, Kleij L, Rabelink T, Weening J, Aten J: Kinetics of connective tissue growth factor expression during experimental proliferative glomerulonephritis. *J Am Soc Nephrol* 12: 472–484, 2001
40. Wahab NA, Brinkman H, Mason RM: Uptake and intracellular transport of the connective tissue growth factor: A potential mode of action. *Biochem J* 359: 89–97, 2001
41. Frazier K, Williams S, Kothapalli D, Klapper H, Grotendorst GR: Stimulation of fibroblast cell growth, matrix production, and granulation tissue formation by connective tissue growth factor. *J Invest Dermatol* 107: 404–411, 1996
42. Chen CC, Mo FE, Lau LF: The angiogenic factor Cyr61 activates a genetic program for wound healing in human skin fibroblasts. *J Biol Chem* 276: 47329–47337, 2001

Effects of Adrenomedullin Inhalation on Hemodynamics and Exercise Capacity in Patients With Idiopathic Pulmonary Arterial Hypertension

Noritoshi Nagaya, MD; Shingo Kyotani, MD; Masaaki Uematsu, MD; Kazuyuki Ueno, PhD; Hideo Oya, MD; Norifumi Nakanishi, MD; Mikiyasu Shirai, MD; Hidezo Mori, MD; Kunio Miyatake, MD; Kenji Kangawa, PhD

Background—Adrenomedullin (AM) is a potent pulmonary vasodilator peptide. However, whether intratracheal delivery of aerosolized AM has beneficial effects in patients with idiopathic pulmonary arterial hypertension remains unknown. Accordingly, we investigated the effects of AM inhalation on pulmonary hemodynamics and exercise capacity in patients with idiopathic pulmonary arterial hypertension.

Methods and Results—Acute hemodynamic responses to inhalation of aerosolized AM (10 μg/kg body wt) were examined in 11 patients with idiopathic pulmonary arterial hypertension during cardiac catheterization. Cardiopulmonary exercise testing was performed immediately after inhalation of aerosolized AM or placebo. The work rate was increased by 15 W/min until the symptom-limited maximum, with breath-by-breath gas analysis. Inhalation of AM produced a 13% decrease in mean pulmonary arterial pressure (54±3 to 47±3 mm Hg, $P<0.05$) and a 22% decrease in pulmonary vascular resistance (12.6±1.5 to 9.8±1.3 Wood units, $P<0.05$). However, neither systemic arterial pressure nor heart rate was altered. Inhalation of AM significantly increased peak oxygen consumption during exercise (peak $\dot{V}O_2$, 14.6±0.6 to 15.7±0.6 mL · kg^{-1} · min^{-1}, $P<0.05$) and the ratio of change in oxygen uptake to that in work rate ($\Delta\dot{V}O_2/\Delta W$ ratio, 6.3±0.4 to 7.0±0.5 mL · min^{-1} · W^{-1}, $P<0.05$). These parameters remained unchanged during placebo inhalation.

Conclusions—Inhalation of AM may have beneficial effects on pulmonary hemodynamics and exercise capacity in patients with idiopathic pulmonary arterial hypertension. (***Circulation.*** **2004;109:351-356.)**

Key Words: peptides ■ hypertension, pulmonary ■ respiration ■ exercise ■ hemodynamics

Idiopathic pulmonary arterial hypertension is a rare but life-threatening disease characterized by progressive pulmonary hypertension, ultimately producing right heart failure and death.[1,2] Although a variety of vasodilators have been proposed as potential therapy for this disease over the past 30 years,[3–7] some patients ultimately require heart-lung or lung transplantation.[8,9] Thus, a novel therapeutic strategy is desirable.

Adrenomedullin (AM) is a potent, long-lasting vasodilator peptide that was originally isolated from human pheochromocytoma.[10] Immunoreactive AM has subsequently been detected in plasma and a variety of tissues, including blood vessels and lungs.[11,12] It has been reported that there are abundant binding sites for AM in the lungs.[13] We have shown that the plasma AM level increases in proportion to the severity of pulmonary hypertension and that circulating AM is partially metabolized in the lungs.[14,15] Interestingly, AM has been shown to inhibit the migration and proliferation of vascular smooth muscle cells.[16,17] These findings suggest that AM plays an important role in the regulation of pulmonary vascular tone and vascular remodeling. In fact, we have shown that short-term intravenous infusion of AM significantly decreases pulmonary vascular resistance in patients with congestive heart failure[18] or pulmonary arterial hypertension.[19] Unfortunately, however, intravenously administered AM induced systemic hypotension in such patients because of nonselective vasodilation in the pulmonary and systemic vascular beds.

More recently, inhalation of aerosolized prostacyclin and its analogue iloprost has been shown to cause pulmonary vasodilation without systemic hypotension in patients with idiopathic pulmonary arterial hypertension.[20,21] In addition, inhalant application of vasodilators does not impair gas exchange because the ventilation-matched deposition of drug

Received February 3, 2003; de novo received July 28, 2003; revision received October 15, 2003; accepted October 19, 2003.

From the Department of Internal Medicine, National Cardiovascular Center, Osaka (N. Nagaya, S.K., H.O., N. Nakanishi, K.M.); the Cardiovascular Division, Kansai Rosai Hospital, Hyogo (M.U.); the Department of Pharmacy, National Cardiovascular Center, Osaka (K.U.); the Department of Cardiac Physiology, National Cardiovascular Center Research Institute, Osaka (M.S., H.M.); and the Department of Biochemistry, National Cardiovascular Center Research Institute, Osaka (K.K.), Japan.

Correspondence to Noritoshi Nagaya, MD, Department of Internal Medicine, National Cardiovascular Center, 5-7-1 Fujishirodai, Suita, Osaka 565-8565, Japan. E-mail nagayann@hsp.ncvc.go.jp

Circulation is available at http://www.circulationaha.org

DOI: 10.1161/01.CIR.0000109493.05849.14

TABLE 1. Baseline Characteristics of Patients With Idiopathic Pulmonary Arterial Hypertension

Demographics	
Age, y	39±3
Male/female, n	2/9
NYHA functional class, n	
III	10
IV	1
Baseline hemodynamics	
MPAP, mm Hg	54±3
CI, $L \cdot min^{-1} \cdot m^{-2}$	2.4±0.1
PVR, Wood units	12.6±1.5
RAP, mm Hg	7±1
PCWP, mm Hg	7±1
Pulmonary function	
Sao_2, %	94±3
Svo_2, %	63±4
FVC, % predicted	86±4
FEV_1, % predicted	75±1
6-Minute walk test, m	355±35
Medication use, n	
Anticoagulant agents	10
Diuretics	9
Digitalis	7
Oral prostacyclin analogue	6
Calcium antagonists	2

NYHA indicates New York Heart Association; MPAP, mean pulmonary arterial pressure; CI, cardiac index; PVR, pulmonary vascular resistance; RAP, mean right atrial pressure; PCWP, pulmonary capillary wedge pressure; Sao_2, arterial oxygen pressure; Svo_2, mixed venous oxygen saturation; FVC, forced vital capacity; and FEV_1, forced expiratory volume in 1 second. Data are mean±SEM.

in the alveoli causes pulmonary vasodilation matched to ventilated areas.[20] In clinical settings, inhalation therapy may be more simple, noninvasive, and comfortable than continuous intravenous infusion therapy. Thus, the purpose of the present study was to investigate the effects of AM inhalation on hemodynamics and exercise capacity in patients with idiopathic pulmonary arterial hypertension.

Methods

Study Subjects

Eleven patients with idiopathic pulmonary arterial hypertension (9 women and 2 men; age, 39±3 years) were included in this study. Idiopathic pulmonary arterial hypertension was defined as pulmonary hypertension unexplained by any secondary cause, on the basis of the criteria of the National Institutes of Health registry.[1] Ten patients were classified as New York Heart Association (NYHA) functional class III and 1 as class IV (Table 1). Two of the 11 patients (18%) were acute responders who showed a significant decrease in mean pulmonary arterial pressure of ≥20% with a decrease in mean pulmonary arterial pressure to <35 mm Hg and no change or an increase in cardiac index during short-term infusion of epoprostenol. Long-term medication, including anticoagulant agents, digitalis, and diuretics, was kept constant. Vasodilator agents, such as oral prostacyclin analogue and calcium antagonists, were stopped ≥12 hours before the study procedure was begun. The ethics committee of the National Cardiovascular Center approved the study, and all patients gave written informed consent.

Preparation of Human AM

Human AM was dissolved in saline with 4% D-mannitol and sterilized by passage through a 0.22-μm filter (Millipore Co). At the time of dispensing, randomly selected vials were submitted for sterility and pyrogen testing. The chemical nature and content of the human AM in vials were verified by high-performance liquid chromatography and radioimmunoassay. All vials were stored frozen at −80°C from the time of dispensing until the time of preparation for administration.

Hemodynamic Studies

Acute hemodynamic responses to AM inhalation were assessed in all patients while they were in a stable condition during hospitalization. Hemodynamic variables, including pulmonary arterial pressure, right atrial pressure, pulmonary capillary wedge pressure, and cardiac output (in triplicate), were determined with a thermodilution catheter (TOO21H-7.5F, Baxter Co).[22] A 22-gauge cannula was inserted into a radial artery for hemodynamic measurements and blood sampling. After an equilibration period of 30 minutes, baseline hemodynamics were measured. Then, AM (10 μg/kg body wt) was inhaled as an aerosol with a jet nebulizer (Porta-Nebu, MEDIC-AID) for 15 minutes, which resulted in a cumulative dose of 400 to 600 μg AM. Hemodynamic parameters were measured at 15-minute intervals starting 15 minutes before AM inhalation until 60 minutes after inhalation. Blood samples for AM measurement were taken at 15-minute intervals from 15 minutes before inhalation until 60 minutes after the end of inhalation.

Cardiopulmonary Exercise Testing

The effects of AM inhalation on exercise capacity were examined in 10 of 11 patients; 1 patient with NYHA class IV underwent the 6-minute walk test according to decision of attending physicians. Cardiopulmonary exercise testing was performed immediately after inhalation of aerosolized AM (10 μg/kg body wt) or saline in a double-blind, randomized, crossover design. This study was performed on 2 separate days, 1 week apart. The first cardiopulmonary exercise testing was performed within 10 days after the cardiac catheterization. The patients performed exercise seated on a cycle ergometer. They first pedaled at 55 rpm without any added load for 1 minute. The work rate was then increased by 15 W/min up to the symptom-limited maximum. Breath-by-breath gas analysis was performed with an AE280 (Minato Medical Science) connected to a personal computer running analyzing software.[23] The ratio of change in oxygen uptake to that in work rate ($\Delta\dot{V}o_2/\Delta W$ ratio) was calculated as the slope of oxygen consumption per unit workload from 1 minute after the start of load addition until 85% maximal $\dot{V}o_2$. Exercise capacity was evaluated by peak oxygen consumption (peak $\dot{V}o_2$), which was defined as the value of averaged data during the final 15 seconds of exercise. Ventilatory efficiency during exercise was represented by the $\dot{V}E$-$\dot{V}co_2$ slope, which was determined as the linear regression slope of $\dot{V}E$ and $\dot{V}co_2$ from the start of exercise until the RC point (the time until which ventilation is stimulated by CO_2 output and end-tidal CO_2 tension begins to decrease).

Measurement of Plasma AM, cAMP, and cGMP

Blood samples were immediately transferred into chilled glass tubes containing disodium EDTA (1 mg/mL) and aprotinin (500 U/mL) and centrifuged immediately at 4°C, and the plasma was frozen and stored at −80°C until assayed. Plasma AM level was measured by a specific immunoradiometric assay kit (Shionogi Pharmaceutical Co Ltd).[24] Plasma cAMP and cGMP were determined with radioimmunoassay kits (cAMP assay kit, cGMP assay kit, Yamasa Shoyu).[18]

Statistical Analysis

All data were expressed as mean±SEM unless otherwise indicated. Changes in hemodynamic and hormonal parameters by AM inhalation were analyzed by 1-way ANOVA for repeated measures,

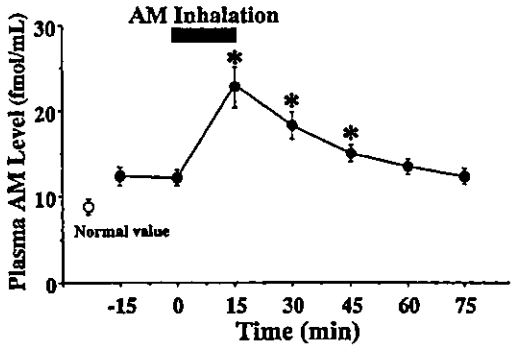

Figure 1. Changes in plasma AM level by inhalation of aerosolized AM in patients with idiopathic pulmonary arterial hypertension. Normal value indicates plasma AM level derived from 15 age-matched healthy subjects. Data are mean±SEM. *$P<0.05$ vs value at time 0.

followed by Newman-Keuls test. Comparisons of exercise parameters between the 2 groups were analyzed with paired Student's t test. A probability value of $P<0.05$ was considered statistically significant.

Results

All patients tolerated this study protocol. One patient developed a headache, and another patient had mild arterial hypoxemia during AM inhalation. None of them experienced other adverse effects, such as systemic hypotension, infection, or arrhythmia.

Plasma AM Level After Inhalation

Baseline plasma AM level in patients with idiopathic pulmonary arterial hypertension was significantly higher than the normal value, which was determined from pooled data of 15 age-matched healthy subjects (11.9±0.8 versus 9.3±0.1 fmol/mL, $P<0.05$). Inhalation of AM significantly increased the plasma AM level to 22.9±2.1 fmol/mL immediately after inhalation (Figure 1). The half-life of plasma AM after inhalation was approximately 20 minutes, and the elevation of AM lasted for >45 minutes. Plasma cAMP level increased significantly 30 minutes after the initiation of AM inhalation (10.8±0.7 to 12.0±0.6 pmol/mL, $P<0.05$), although plasma cGMP level was not significantly altered (6.5±1.0 to 6.8±1.0 pmol/mL, P=NS).

Hemodynamic Effects of AM Inhalation

Inhalation of AM significantly decreased mean pulmonary arterial pressure in patients with idiopathic pulmonary arterial hypertension (54±3 to 47±3 mm Hg, $P<0.05$) without a significant decrease in mean arterial pressure (85±4 to 83±4 mm Hg, P=NS) (Figure 2). AM inhalation slightly but significantly increased cardiac index by 12% (2.4±0.1 to 2.7±0.2 L · min^{-1} · m^{-2}, $P<0.05$). Thus, AM inhalation resulted in a 22% decrease in pulmonary vascular resistance (12.6±1.5 to 9.8±1.3 Wood units, $P<0.05$) (Figure 3). Inhaled AM did not significantly alter systemic vascular resistance. The ratio of pulmonary vascular resistance to systemic vascular resistance was decreased significantly at the end of inhalation (0.63±0.08 to 0.55±0.07, $P<0.05$). These hemodynamic effects of AM lasted for >45 minutes.

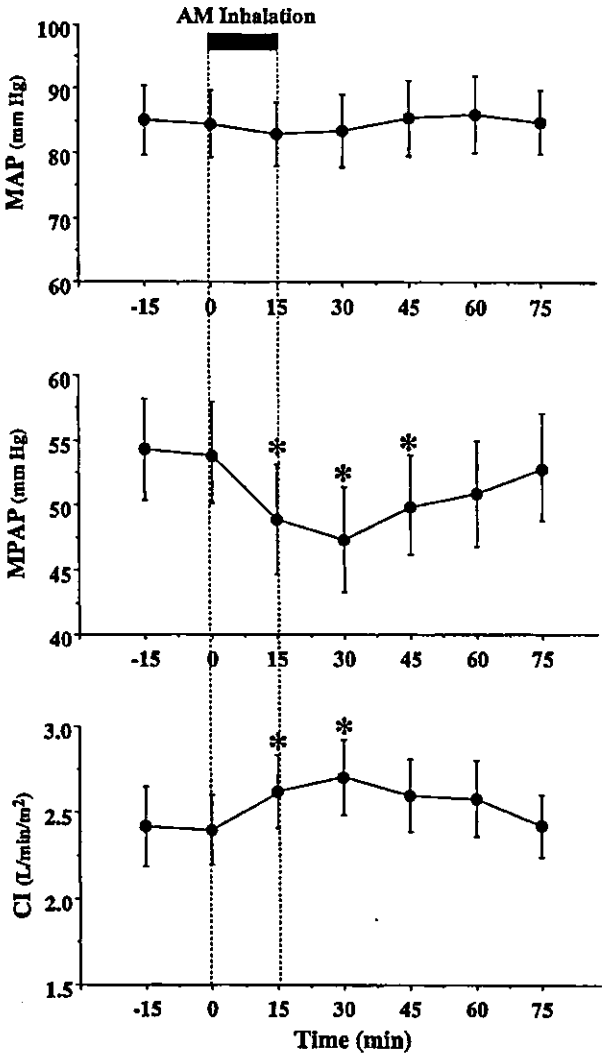

Figure 2. Changes in mean arterial pressure (MAP), mean pulmonary arterial pressure (MPAP), and cardiac index (CI) by inhalation of aerosolized AM in patients with idiopathic pulmonary arterial hypertension. Data are mean±SEM. *$P<0.05$ vs value at time 0.

No significant change in heart rate, pulmonary capillary wedge pressure, or right atrial pressure was observed. There was no significant change in arterial oxygen saturation (94±3% to 93±3%).

Effects of AM Inhalation on Exercise Capacity and Ventilatory Efficiency

As the limiting symptom at the end of exercise, 6 patients reported muscle weakness and 4 reported dyspnea. There was no difference in these symptoms when exercise testing was performed with or without inhalation of AM. Inhalation of AM altered neither heart rate nor blood pressure either at rest or at peak exercise (Table 2). Inhalation of AM significantly increased peak workload (86±5 to 93±6 W, $P<0.05$) (Table 2). AM also significantly increased peak $\dot{V}o_2$ (14.6±0.6 to 15.7±0.6 mL · kg^{-1} · min^{-1}, $P<0.05$) (Figure 4). Inhalation of AM significantly increased $\Delta\dot{V}o_2/\Delta W$ ratio (6.3±0.4 to

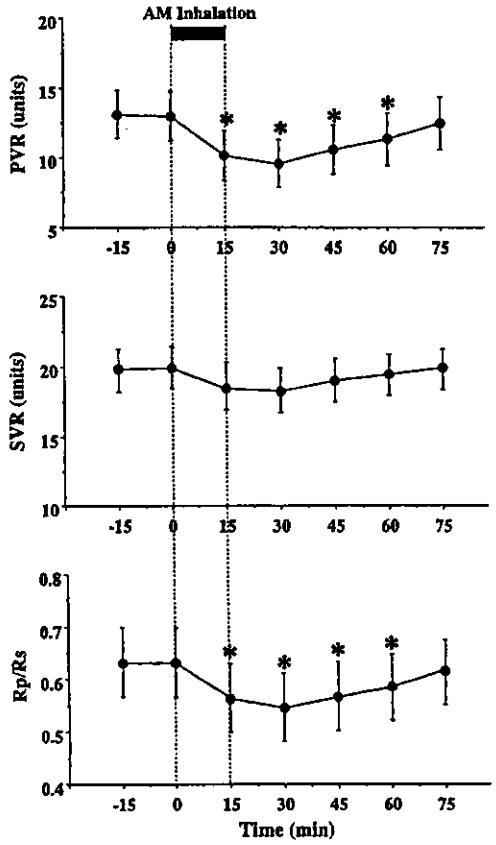

Figure 3. Changes in pulmonary vascular resistance (PVR), systemic vascular resistance (SVR), and ratio of pulmonary vascular resistance to systemic vascular resistance (Rp/Rs) by inhalation of aerosolized AM in patients with idiopathic pulmonary arterial hypertension. Data are mean±SEM. *$P<0.05$ vs value at time 0.

7.0 ± 0.5 mL · min^{-1} · W^{-1}, $P<0.05$). AM did not significantly alter the $\dot{V}_E$-$\dot{V}_{CO_2}$ slope (Table 2). No significant changes in arterial oxygen saturation were observed either at rest or at peak exercise. In 1 patient with NYHA class IV who did not undergo cardiopulmonary exercise testing, the distance walked in 6 minutes increased from 150 to 180 m by inhalation of AM.

Discussion

In the present study, we demonstrated that inhalation of AM improved hemodynamics with pulmonary selectivity and exercise capacity in patients with idiopathic pulmonary arterial hypertension.

AM is one of the most potent endogenous vasodilators in the pulmonary vascular bed.[25–27] The vasodilatory effect is mediated by cAMP-dependent and nitric oxide–dependent mechanisms.[28,29] Endogenous AM production is enhanced in a variety of cardiovascular diseases through a compensatory mechanism.[14,30] Nonetheless, additional supplementation of AM has beneficial effects in these diseases.[18,19] These results suggest that endogenous AM level is not sufficient to improve deteriorated conditions despite the increased AM production. Interestingly, Champion et al[31] have shown that intratracheal gene transfer of calcitonin gene–related peptide, a member of the same peptide family as AM, to bronchial

TABLE 2. Changes in Exercise Parameters by Inhalation of AM or Placebo

Variables	Placebo	AM	*P*
Peak workload, W	86±5	93±6	<0.05
HR, bpm			
Rest	75±5	75±3	NS
Peak	144±6	148±6	NS
MAP, mm Hg			
Rest	85±3	87±5	NS
Peak	108±5	110±6	NS
Peak Borg score (D/L)	17/18	18/18	NS
Peak $\dot{V}o_2$, mL · kg^{-1} · min^{-1}	14.6±0.6	15.7±0.6	<0.05
$\Delta\dot{V}o_2/\Delta W$ ratio, mL · min^{-1} · W^{-1}	6.3±0.4	7.0±0.5	<0.05
$\dot{V}_E$-$\dot{V}_{CO_2}$ slope	37±2	36±2	NS
Sao_2, %			
Rest	97±1	97±1	NS
Peak	95±1	95±1	NS

HR indicates heart rate; MAP, mean arterial pressure; Peak Borg score (D/L), Borg score at peak exercise (dyspnea/leg fatigue); Peak $\dot{V}o_2$, peak oxygen consumption; $\Delta\dot{V}o_2/\Delta W$ ratio, $\dot{V}o_2$ increase per unit workload; $\dot{V}_E$-$\dot{V}_{CO_2}$ slope, slope of regression line of relation between $\dot{V}_E$ and $\dot{V}_{CO_2}$; and Sao_2, arterial oxygen saturation. Data are mean±SEM.

epithelial cells attenuates chronic hypoxia-induced pulmonary hypertension in the mouse. These results raise the possibility that intratracheal delivery of a vasodilator peptide may be sufficient to alter pulmonary vascular function. In fact, in the present study, inhalation of AM significantly decreased pulmonary vascular resistance, whereas it did not alter systemic arterial pressure or systemic vascular resistance. The ratio of pulmonary vascular resistance to systemic vascular resistance was reduced significantly by AM inhalation. These results suggest that inhaled AM improves hemodynamics with pulmonary selectivity. This is consistent with earlier findings that inhaled prostacyclin or its analogue iloprost acts transepithelially with pulmonary selectivity and improves pulmonary hypertension.[20,21] Inhalation of AM slightly but significantly increased cardiac index in patients with idiopathic pulmonary arterial hypertension. Considering the strong vasodilator activity of AM in the pulmonary vasculature, the significant decrease in cardiac afterload may be responsible for increased cardiac index with

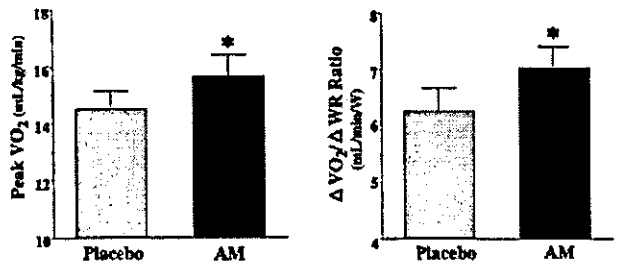

Figure 4. Changes in peak oxygen consumption (peak $\dot{V}o_2$) and ratio of change in oxygen uptake to that in work rate ($\Delta\dot{V}o_2/\Delta W$ ratio) by inhalation of aerosolized AM or placebo in patients with idiopathic pulmonary arterial hypertension. Data are mean±SEM. *$P<0.05$ vs placebo.

AM. Interestingly, the hemodynamic effects of inhaled AM lasted for >45 minutes. A previous study demonstrated that intravenous injection of AM produces a long-lasting vasodilator response because of its long half-life (≈15 minutes).[32] The half-life of plasma AM after inhalation was longer (20 minutes). Thus, inhalation of AM may cause relatively long-lasting pulmonary vasodilator activity in patients with idiopathic pulmonary arterial hypertension. In the present study, plasma cAMP level increased after AM inhalation, suggesting that the hemodynamic effects of AM may be mediated by activation of cAMP.

Earlier studies have shown that peak $\dot{V}O_2$ during exercise is markedly lower in patients with idiopathic pulmonary arterial hypertension than in healthy subjects.[33,34] Peak $\dot{V}O_2$ is determined primarily by the maximal cardiac output during exercise and the potential for O_2 extraction by the exercising muscle.[35] Thus, the decreased peak $\dot{V}O_2$ may reflect insufficient oxygen delivery to the body during exercise, at least in part because of an inadequate increase in cardiac output under conditions of severe pulmonary hypertension. In the present study, inhalation of AM significantly increased peak $\dot{V}O_2$ in patients with pulmonary hypertension. AM also increased the $\Delta\dot{V}O_2/\Delta W$ ratio, which indicates oxygen transport per unit workload to the exercising legs. These results suggest that inhalation of AM improves exercise capacity in patients with idiopathic pulmonary arterial hypertension. It is possible that an increase in cardiac output during exercise may contribute to increases in peak $\dot{V}O_2$ and the $\Delta\dot{V}O_2/\Delta W$ ratio.

The major limitation of this pilot trial relates to the lack of a randomized, placebo-controlled group in acute hemodynamic studies, which was as result not only of invasive assessment of hemodynamics but also of the limited number of patients available. Nevertheless, cardiopulmonary exercise testing was performed in a double-blind, randomized, crossover design. Thus, it is unlikely that the hemodynamic effects of inhaled AM are attributable to the placebo effect.

Inhalation therapy may be more simple, noninvasive, and comfortable than continuous intravenous infusion therapy. An experimental study demonstrated that repeated inhalation of AM (for 30 minutes, 4 times a day) inhibited monocrotaline-induced pulmonary hypertension and markedly improved survival in rats.[36] Recently, pulmonary delivery of a dry-powder insulin has been shown to improve glycemic control without adverse pulmonary effects.[37] Although further studies are necessary to maximize the efficiency and reproducibility of pulmonary AM delivery, combining AM inhalation therapy with other modalities that have a different mode of action may have beneficial effects in patients with idiopathic pulmonary arterial hypertension.

Conclusions

These preliminary results suggest that inhalation of AM may have beneficial effects on pulmonary hemodynamics and exercise capacity in patients with idiopathic pulmonary arterial hypertension.

Acknowledgments

This work was supported by grants from NEDO, the Mochida Memorial Foundation for Medical and Pharmaceutical Research, the Japan Cardiovascular Research Foundation, Health and Labor Sciences Research grant genome 005, and the Promotion of Fundamental Studies in Health Science of the Organization for Pharmaceutical Safety and Research of Japan. We thank Masahiko Shibakawa for preparing AM.

References

1. Rich S, Dantzker DR, Ayres SM, et al. Primary pulmonary hypertension: a national prospective study. *Ann Intern Med.* 1987;107:216–223.
2. Rich S. Primary pulmonary hypertension. *Prog Cardiovasc Dis.* 1988;31: 205–238.
3. Rubin LJ, Peter RH. Oral hydralazine therapy for primary pulmonary hypertension. *N Engl J Med.* 1980;302:69–73.
4. Rich S, Kaufmann E, Levy PS. The effect of high doses of calcium-channel blockers on survival in primary pulmonary hypertension. *N Engl J Med.* 1992;327:76–81.
5. Barst RJ, Rubin LJ, Long WA, et al. A comparison of continuous intravenous epoprostenol (prostacyclin) with conventional therapy for primary pulmonary hypertension. *N Engl J Med.* 1996;334:296–301.
6. McLaughlin VV, Genthner DE, Panella MM, et al. Reduction in pulmonary vascular resistance with long-term epoprostenol (prostacyclin) therapy in primary pulmonary hypertension. *N Engl J Med.* 1998;338:273–277.
7. Nagaya N, Uematsu M, Okano Y, et al. Effect of orally active prostacyclin analogue on survival of outpatients with primary pulmonary hypertension. *J Am Coll Cardiol.* 1999;34:1188–1192.
8. Reitz BA, Wallwork JL, Hunt SA, et al. Heart-lung transplantation: successful therapy for patients with pulmonary vascular disease. *N Engl J Med.* 1982;306:557–564.
9. Pasque MK, Trulock EP, Kaiser LD, et al. Single lung transplantation for pulmonary hypertension: three month hemodynamic follow-up. *Circulation.* 1991;84:2275–2279.
10. Kitamura K, Kangawa K, Kawamoto M, et al. Adrenomedullin: a novel hypotensive peptide isolated from human pheochromocytoma. *Biochem Biophys Res Commun.* 1993;192:553–560.
11. Ichiki Y, Kitamura K, Kangawa K, et al. Distribution and characterization of immunoreactive adrenomedullin in human tissue and plasma. *FEBS Lett.* 1994;338:6–10.
12. Sakata J, Shimokubo T, Kitamura K, et al. Distribution and characterization of immunoreactive rat adrenomedullin in tissue and plasma. *FEBS Lett.* 1994;352:105–108.
13. Owji AA, Smith DM, Coppock HA, et al. An abundant and specific binding site for the novel vasodilator adrenomedullin in the rat. *Endocrinology.* 1995;136:2127–2134.
14. Kakishita M, Nishikimi T, Okano Y, et al. Increased plasma levels of adrenomedullin in patients with pulmonary hypertension. *Clin Sci.* 1999;96: 33–39.
15. Yoshibayashi M, Kamiya T, Kitamura K, et al. Plasma levels of adrenomedullin in primary and secondary pulmonary hypertension in patients < 20 years of age. *Am J Cardiol.* 1997;79:1556–1558.
16. Horio T, Kohno M, Kano H, et al. Adrenomedullin as a novel antimigration factor of vascular smooth muscle cells. *Circ Res.* 1995;77:660–664.
17. Kano H, Kohno M, Yasunari K, et al. Adrenomedullin as a novel antiproliferative factor of vascular smooth muscle cells. *J Hypertens.* 1996;14: 209–213.
18. Nagaya N, Satoh T, Nishikimi T, et al. Hemodynamic, renal, and hormonal effects of adrenomedullin infusion in patients with congestive heart failure. *Circulation.* 2000;101:498–503.
19. Nagaya N, Nishikimi T, Uematsu M, et al. Haemodynamic and hormonal effects of adrenomedullin in patients with pulmonary hypertension. *Heart.* 2000;84:653–658.
20. Walmrath D, Schneider T, Pilch J, et al. Aerosolized prostacyclin reduces pulmonary artery pressure and improves gas exchange in the adult respiratory distress syndrome (ARDS). *Lancet.* 1993;342:961–962.
21. Hoeper MM, Schwarze M, Ehlerding S, et al. Long-term treatment of primary pulmonary hypertension with aerosolized iloprost, a prostacyclin analogue. *N Engl J Med.* 2000;342:1866–1870.
22. Rich S, Seidlitz M, Dodin E, et al. The short-term effects of digoxin in patients with right ventricular dysfunction from pulmonary hypertension. *Chest.* 1998;114:787–792.
23. Miyamoto S, Nagaya N, Satoh T, et al. Clinical correlates and prognostic significance of six-minute walk test in patients with primary pulmonary

hypertension: comparison with cardiopulmonary exercise testing. *Am J Respir Crit Care Med.* 2000;161:487–492.
24. Ohta H, Tsuji T, Asai S, et al. A simple immunoradiometric assay for measuring the entire molecules of adrenomedullin in human plasma. *Clin Chim Acta.* 1999;287:131–143.
25. Lippton H, Chang JK, Hao Q, et al. Adrenomedullin dilates the pulmonary vascular bed in vivo. *J Appl Physiol.* 1994;76:2154–2156.
26. Heaton J, Lin B, Chang JK, et al. Pulmonary vasodilation to adrenomedullin: a novel peptide in humans. *Am J Physiol.* 1995;268:H2211–H2215.
27. Nossaman BD, Feng CJ, Kaye AD, et al. Pulmonary vasodilator responses to adrenomedullin are reduced by NOS inhibitors in rats but not in cats. *Am J Physiol.* 1996;270:L782–L789.
28. Ishizaka Y, Ishizaka Y, Tanaka M, et al. Adrenomedullin stimulates cyclic AMP formation in rat vascular smooth muscle cells. *Biochem Biophys Res Commun.* 1994;200:642–646.
29. Nakamura M, Yoshida H, Makita S, et al. Potent and long-lasting vasodilatory effects of adrenomedullin in humans: comparisons between normal subjects and patients with chronic heart failure. *Circulation.* 1997;95: 1214–1221.
30. Nagaya N, Nishikimi T, Yoshihara F, et al. Cardiac adrenomedullin gene expression and peptide accumulation after acute myocardial infarction in rats. *Am J Physiol.* 2000;278:R1019–R1026.
31. Champion HC, Bivalacqua TJ, Toyoda K, et al. In vivo gene transfer of prepro-calcitonin gene-related peptide to the lung attenuates chronic hypoxia-induced pulmonary hypertension in the mouse. *Circulation.* 2000;101: 931–937.
32. Ishiyama Y, Kitamura K, Ichiki Y, et al. Haemodynamic responses to rat adrenomedullin in anaesthetized spontaneously hypertensive rats. *Clin Exp Pharmacol Physiol.* 1995;22:614–618.
33. D'Alonzo GE, Gianotti LA, Pohil RL, et al. Comparison of progressive exercise performance of normal subjects and patients with primary pulmonary hypertension. *Chest.* 1987;92:57–62.
34. Wensel R, Opitz CF, Anker SD, et al. Assessment of survival in patients with primary pulmonary hypertension: importance of cardiopulmonary exercise testing. *Circulation.* 2002;106:319–324.
35. Anderson P, Saltin B. Maximal perfusion of skeletal muscle in man. *J Appl Physiol.* 1985;366:233–249.
36. Nagaya N, Okumura H, Uematsu M, et al. Repeated inhalation of adrenomedullin ameliorates pulmonary hypertension and survival in monocrotaline rats. *Am J Physiol Heart Circ Physiol.* 2003;285:H2125–H2131.
37. Skyler JS, Cefalu WT, Kourides IA, et al. Efficacy of inhaled human insulin in type 1 diabetes mellitus: a randomised proof-of-concept study. *Lancet.* 2001;357:331–335.

Adrenomedullin Infusion Attenuates Myocardial Ischemia/Reperfusion Injury Through the Phosphatidylinositol 3-Kinase/Akt-Dependent Pathway

Hiroyuki Okumura, MD; Noritoshi Nagaya, MD; Takefumi Itoh, MD; Ichiro Okano, PhD; Jun Hino, PhD; Kenji Mori, PhD; Yoshitane Tsukamoto, MD; Hatsue Ishibashi-Ueda, MD; Senri Miwa, MD; Keiichi Tambara, MD; Shinya Toyokuni, MD; Chikao Yutani, MD; Kenji Kangawa, PhD

Background—Infusion of adrenomedullin (AM) has beneficial hemodynamic effects in patients with heart failure. However, the effect of AM on myocardial ischemia/reperfusion remains unknown.

Methods and Results—Male Sprague-Dawley rats were exposed to a 30-minute period of ischemia induced by ligation of the left coronary artery. They were randomized to receive AM, AM plus wortmannin (a phosphatidylinositol 3-kinase [PI3K] inhibitor), or saline for 60 minutes after coronary ligation. Hemodynamics and infarct size were examined 24 hours after reperfusion. Myocardial apoptosis was also examined 6 hours after reperfusion. The effect of AM on Akt phosphorylation in cardiac tissues was examined by Western blotting. Intravenous administration of AM significantly reduced myocardial infarct size (28±4% to 16±1%, $P<0.01$), left ventricular end-diastolic pressure (19±2 to 8±2 mm Hg, $P<0.05$), and myocardial apoptotic death (19±2% to 9±4%, $P<0.05$). Western blot analysis showed that AM infusion accelerated Akt phosphorylation in cardiac tissues and that pretreatment with wortmannin significantly attenuated AM-induced Akt phosphorylation. Moreover, pretreatment with wortmannin abolished the beneficial effects of AM: a reduction of infarct size, a decrease in left ventricular end-diastolic pressure, and inhibition of myocardial apoptosis after ischemia/reperfusion.

Conclusions—Short-term infusion of AM significantly attenuated myocardial ischemia/reperfusion injury. These cardioprotective effects are attributed mainly to antiapoptotic effects of AM via a PI3K/Akt-dependent pathway. **(*Circulation*. 2004;109:242-248.)**

Key Words: peptides ■ reperfusion ■ apoptosis ■ myocardial infarction ■ hemodynamics

Coronary revascularization has been established as the most effective treatment for coronary artery disease. However, reperfusion can elicit a number of adverse reactions that may limit its beneficial actions. Although it has been attempted to reduce ischemia/reperfusion injury in many basic or clinical studies, few agents are clinically available for ischemia/reperfusion injury.

Adrenomedullin (AM) is a potent vasodilatory peptide that was originally isolated from human pheochromocytoma.[1] We have shown that AM peptide and mRNA are distributed in the heart[2,3] and that plasma and cardiac AM markedly increase after acute myocardial infarction.[4,5] AM has been shown to be a possible endogenous suppressor of myocyte hypertrophy[6] and fibroblast proliferation.[7] In addition, intravenous infusion of AM has beneficial hemodynamic effects in patients with heart failure.[8] These findings suggest that AM induces cardioprotective effects not only as a circulating factor but also as a paracrine and/or autocrine factor.

Recently, AM has been shown to activate the Akt pathway in vascular endothelial cells.[9] Interestingly, the Akt activation has been reported to lead to the prevention of myocardial injury after transient ischemia in vivo through antiapoptotic effects.[10] However, whether AM, a potent Akt activator, attenuates myocardial ischemia/reperfusion injury remains unknown.

Thus, the purposes of this study were (1) to investigate whether short-term infusion of AM reduces myocardial infarct size, inhibits myocyte apoptosis, and thereby improves cardiac function after ischemia/reperfusion and (2) to determine whether the underlying mechanisms are associated with

Received January 27, 2003; de novo received August 11, 2003; accepted September 22, 2003.

From the Department of Biochemistry (H.O., I.O., J.H., K.M., K.K.), National Cardiovascular Center Research Institute, Osaka, Japan; Department of Internal Medicine (N.N., T.I.) and Department of Pathology (Y.T., H.I.-U., C.Y.), National Cardiovascular Center, Osaka, Japan; and Department of Cardiovascular Surgery (S.M., K.T.) and Department of Pathology and Biology of Diseases (S.T.), Graduate School of Medicine, Kyoto University, Kyoto, Japan.

Correspondence to Noritoshi Nagaya, MD, National Cardiovascular Center, 5-7-1 Fujishirodai, Suita, Osaka 565-8565, Japan. E-mail nagayann@hsp.ncvc.go.jp

Circulation is available at http://www.circulationaha.org

DOI: 10.1161/01.CIR.0000109214.30211.7C